Scilight

Applied Energy Science

https://www.sciltp.com/journals/aes

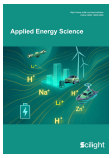

Review

Phosphoric Acid-Doped Polymer Electrolyte Membranes for High-Temperature Proton Exchange Membrane Fuel Cells: Actualities and Perspective

Yu Bai [1], Dongmei Han [1,2], Sheng Huang [1], Min Xiao [1] and Shuanjin Wang [1,*]

[1] The Key Laboratory of Low-carbon Chemistry & Energy Conservation of Guangdong Province/State Key Laboratory of Optoelectronic Materials and Technologies, Sun Yat-sen University, Guangzhou 510275, China
[2] School of Chemical Engineering and Technology, Sun Yat-sen University, Zhuhai 519082, China
* Correspondence: wangshj@mail.sysu.edu.cn; 020-84115506

How To Cite: Bai, Y.; Han, D.; Huang, S.; et al. A Phosphoric Acid-Doped Polymer Electrolyte Membranes for High-Temperature Proton Exchange Membrane Fuel Cells: Actualities and Perspective. *Applied Energy Science* **2026**, *1*(1), 2.

Received: 29 December 2025
Revised: 10 March 2026
Accepted: 16 March 2026
Published: 26 March 2026

Abstract: Proton exchange membrane fuel cells (PEMFCs) offer a promising solution for power generation, boasting higher efficiency than traditional coal combustion engines and a more environmentally friendly design. Proton exchange membranes play a crucial role in determining the overall performance of PEMFCs. Significant efforts have been dedicated to this area, resulting in the development of innovative material systems. Membranes employing phosphoric acid (PA) as the proton conductor currently dominate the field of high-temperature proton exchange membranes operating in the temperature range of 100~200 °C. This paper aims to provide a concise overview of high-temperature proton exchange membranes (HT-PEMs) to aid researchers in obtaining essential information efficiently. The proton conduction and fundamental principles, recent research efforts and limitations, as well as the challenges and promising directions for future advancements of PA-dependent HT-PEMs are summarized.

Keywords: fuel cell; high-temperature proton exchange membrane; phosphoric acid; polybenzimidazole

1. Introduction

Proton exchange membrane fuel cells (PEMFCs) have garnered considerable attention for fuel-cell vehicles owing to their high efficiency, fast start-up and low environmental impact. Compared with emerging alternative technologies, PEMFCs present distinct advantages in high-temperature tolerance, fuel flexibility and long-duration energy supply. However, performance and durability issues remain critical for large-scale commercialization, highlighting the significance of continuous research in this field [1–4]. The core component of a PEMFC is known as the membrane electrode assembly (MEA), which is comprised of the central proton exchange membrane, flanked by the catalyst layers and gas diffusion layers on both the anode and cathode sides. The perfluorinated sulfonic acid (PFSA) membrane, notably represented by the DuPont Nafion series, currently dominates the landscape of proton exchange membranes in both research and commercial applications. Nonetheless, the proton conduction of perfluorinated sulfonic acid membranes is reliant on water, restricting their application to temperatures below 80 °C, hindering the enhancement of electrode reaction kinetics and power density outputs [5–8]. In recent years, there has been a growing interest in high-temperature proton exchange membrane fuel cells (HT-PEMFCs) utilizing phosphoric acid (PA) as the proton conductor. Phosphoric acid exhibits low volatility, and undergoes self-ionization at elevated temperatures and anhydrous conditions, enabling the operation of such proton exchange membranes in an anhydrous environment within the temperature range of 100~200 °C [9–12]. It is noted that the term “HT-PEMFCs” is used in relation to low-temperature proton exchange membrane fuel cells (LT-PEMFCs) operating below 80 °C, in comparison, HT-PEMFCs afford the following advantages: (i) Facilitated gas transport

and electrocatalytic reactivity; (ii) Enhanced tolerance of the catalyst to CO (the adsorption of CO on Pt is negligible at 140 °C); (iii) Simplified humidity system and cooling system [13–17].

Phosphoric acid-doped polybenzimidazole (PA/PBIs) represents a benchmark for high-temperature proton exchange membranes (HT-PEMs). PBI exhibits outstanding heat resistance, high mechanical performance, and chemical stability. In HT-PEMFCs operating at 160 °C without additional humidification, PA/PBIs enables a service life exceeding 10,000 h [18]. A number of literatures revolve around the modification of polybenzimidazole-based HT-PEM. Several PBI structures reported in the literature are depicted in Figure 1.

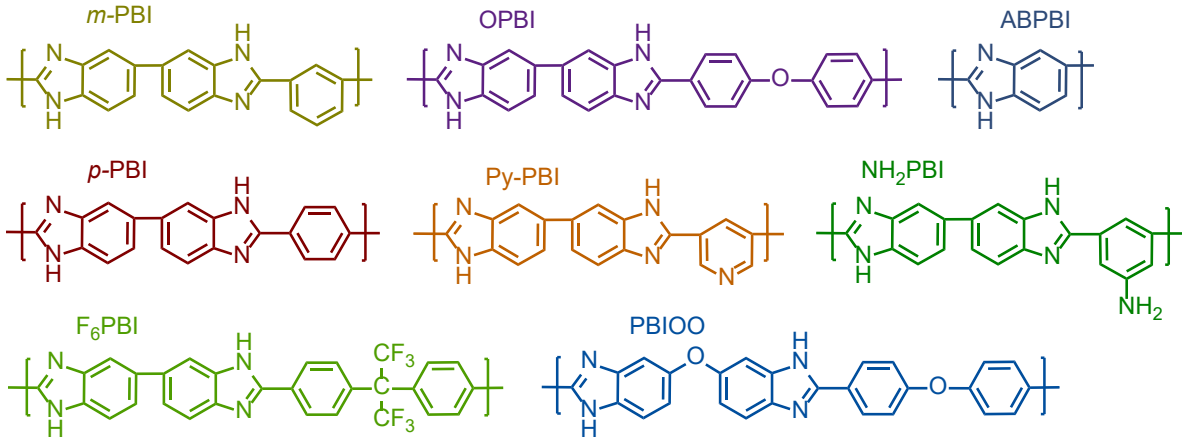

Figure 1. Summary of most commonly reported PBI backbones.

Polybenzimidazole acts as a strong Brönsted base with respect to neat phosphoric acid, benzimidazole's nitrogen can be fully protonated, leading to the formation of "strongly bound PA". Simultaneously, phosphoric acid molecules can form extensive "loosely bound" PA or "free PA" through hydrogen bonding interactions with the polymer and other phosphoric acid molecules [19,20]. For descriptions of phosphoric acid content in HT-PEM, one can calculate the molecular ratio of PA to polybenzimidazole repeat unit (Equation (1)), or the percentage of phosphoric acid mass adsorbed on the dry membrane mass (Equation (2)).

$$\mathrm{ADL} = \frac{m_W - m_D}{M_{PA} \times (m_D / M_{\mathrm{PBI}})} \tag{1}$$

$$\mathrm{PA\ uptake}(\%) = \frac{m_W - m_D}{m_D} \times 100\% \tag{2}$$

where m_W and m_D are the masses of the PA-doped and PA-undoped membranes, respectively, M_{PA} and M_{PBI} are the molecular weights of PA and PBI repeating unit, respectively.

Within PA/PBI, the rapid proton conduction is resulted from a frustrated hydrogen-bond network, protons hop through the stretching vibrations of hydrogen-bond from one proton carrier to an adjacent proton carrier, allowing the former to accept protons again, thereby establishing a dynamic and continuous transfer of protons. This mechanism is known as the Grotthuss mechanism [11,21–23]. Figure 2 illustrates the schematic depiction of the proton transfer mechanism in PA-doped PBI electrolyte membranes. Ma et al. [23] have proposed that the exchange rate of protons among different molecules is as follows: PA–water > PA–PA > imidazole–PA > imidazole–water > imidazole–imidazole. The proton exchange rate between protonated imidazole and dihydrogen phosphate is relatively low, therefore, the diffusion and conduction of protons are predominantly reliant on the hydrogen bonding network of free PA [19,23].

Literature reports often involve a significant doping of phosphoric acid, this is contributed to the presence of free acid. The amount of free acid not only significantly impacts the volume swelling, but also dictates the proton conductivity [24–26]. However, elevated acid doping levels can cause significant dimensional expansion and compromise mechanical integrity. Hence, an extensive scholarly discourse is dedicated to the optimization of overall performance of PEMs. As a fundamental principle in the construction of PA-dependent HT-PEMs, alkaline moieties such as benzimidazoles, pyridines, triazoles, imides, amides, and quaternary ammonium are introduced via covalently bonding or doping/blending techniques into the polymer matrix. This approach endows the membranes with processability and phosphoric acid adsorption capacity. This review aims to offer a concise yet comprehensive overview of the advancements in understanding and design considerations of PA-doped

membranes in recent years. We will categorize HT-PEMs into single-component polymer membranes and composite membranes, as illustrated in Figure 3.

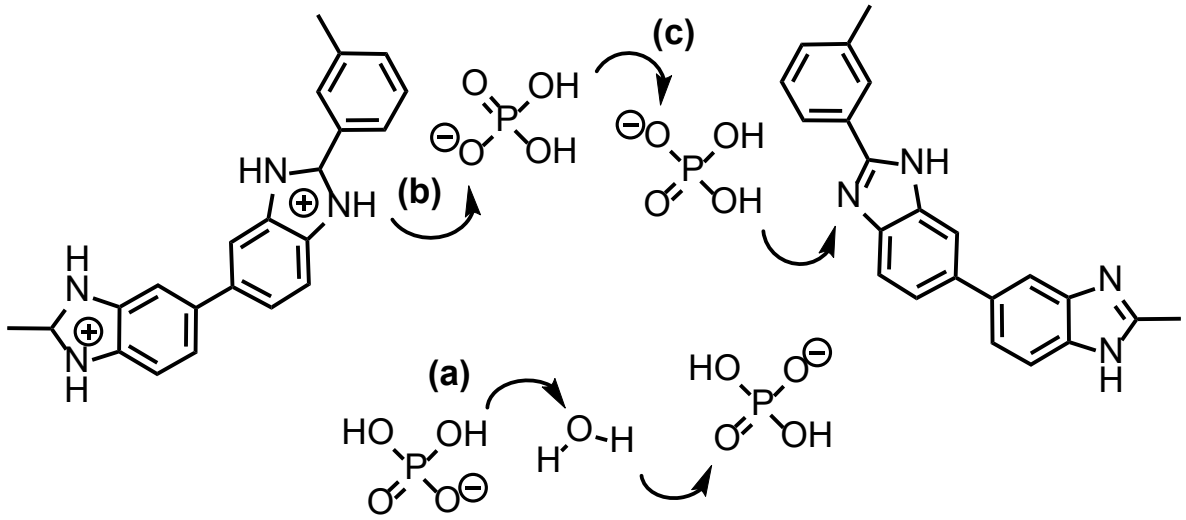

Figure 2. Primary proton conducting pathways in PA/PBI membranes: (**a**) PA–water proton transfer; (**b**) PA–PA proton transfer; (**c**) benzimidazole–PA proton transfer [27], Copyright 2014, John Wiley and Sons.

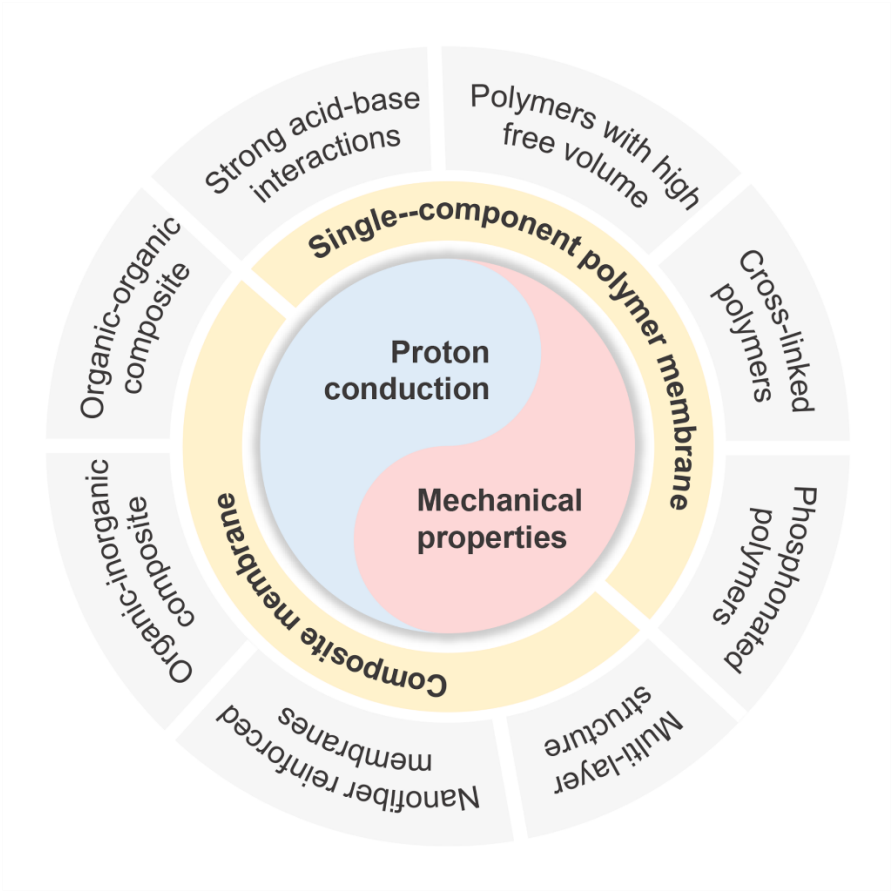

Figure 3. Schematic illustration of formation technique of HT-PEMs.

2. Single-Component Polymer Membranes

From a structural design perspective, the single-component polymer membrane is categorized into four segments—strong acid-base interactions, polymers with high free volume, cross-linked polymers, and phosphonated polymers—for detailed examination, some representative well-designed structures and the corresponding key performance parameters are summarized in Table 1.

Table 1. Key performance parameters of some homogenous high-temperature proton exchange membranes.

Membrane	PA Uptake (%)	Proton Conductivity (mS cm^{-1})	Fracture Stress (MPa)	Peak Power Density* (mW cm^{-2})	Chemical structure
TDAP-PSU-88 [28]	186	<50	~2.0	453 (150 °C)	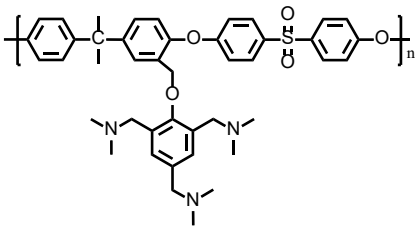
g-PBI-20 [29]	ADL = 22.1	212 (200 °C)	6.5	443	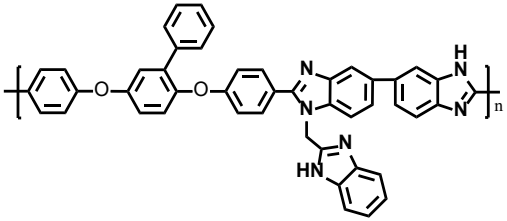
QPAF-4 [30]	150	52	10.3	683	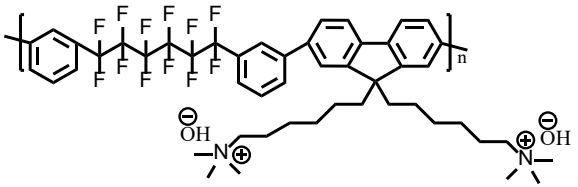
DMBP-TB/PA [31]	425	144	/	815	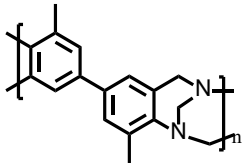
OPBI-R2-9 [32]	ADL = 10.5	53 (180 °C)	~8.0	222 (H_2/air)	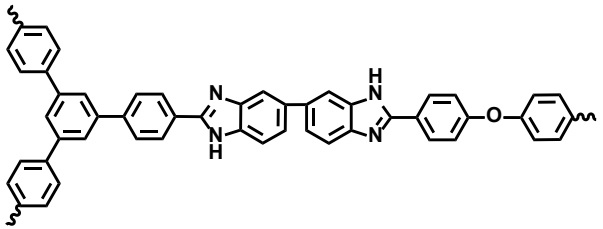

Table 1. *Cont.*

Membrane	PA Uptake (%)	Proton Conductivity (mS cm^{-1})	Fracture Stress (MPa)	Peak Power Density* (mW cm^{-2})	Chemical structure
Br*p*PBI-*b*-F6-PBI [33]	ADL = 17.5	150	2.9	713	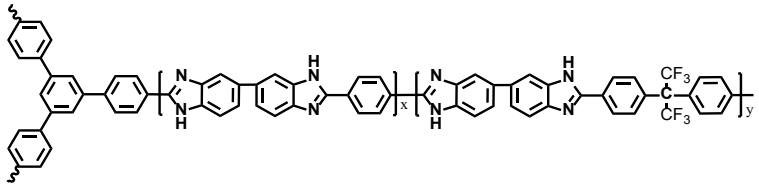
QOPBI-15 [34]	167	49	27.0	260 (H_2/air)	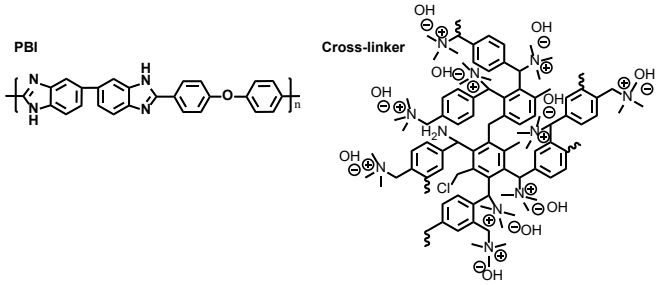
C10F6-R2-6 [35]	~230	73	14.0	690	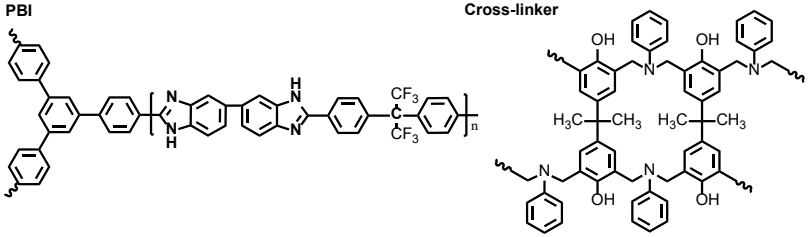
OPBI-CL-Pillar-7% [36]	316	116	14.6	1084 (180 °C)	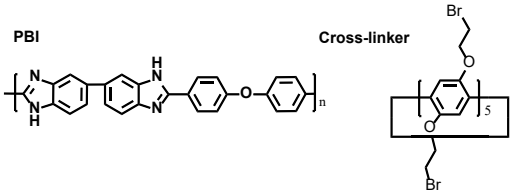
P/PITP-20 [37]	90	99	~14.0	812	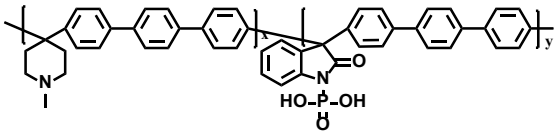

* H_2/O_2 fuel cell performances (160 °C).

2.1. Strong Acid-Base Interactions

High-temperature proton exchange membranes are essentially acid-base composite membranes. By increasing the equivalent of basic groups, the affinity of matrix to acid molecules can be enhanced, thus elevating the phosphoric acid doping content and retention ability; introducing strong alkaline functional groups can promote the dissociation of phosphoric acid, forming strong ion pairs and thereby immobilizing the phosphoric acid [38–40].

Zhang et al. [28] grafted 2,4,6-tri(dimethylaminomethyl)-phenol (TDAP) with three tertiary amine groups onto polysulfone (PSU), increasing the number of basic groups on side chains and the interactions between PA molecules and the membranes. The TDAP-PSU membrane with 88% grafting degree achieved a PA uptake of 186%, single cell based on this membrane reached a peak power density of 453 mW cm^{-2} at 150 °C. The stability of the PA-doped TDAP-PSU-88 membrane was evaluated at a constant voltage of 0.6 V without additional humidification. The cell remained stable with no performance decay during continuous operation at 150 °C for more than 70 h. Liu et al. [29] grafted benzimidazole onto an arylether-type polybenzimidazole by N-substitution reaction, the introduction of additional benzimidazole moieties greatly increased the PA doping level per unit volume. With a grafting degree of 20% and an ADL of 22.1, the *g*-PBI-20 membrane exhibited a proton conductivity of 212 mS cm^{-1} at 200 °C and a peak power density of 443 mW cm^{-2} at 160 °C.

Yang et al. synthesized a series of pyridine-containing poly(triphenyl-co-dibenzo-18-crown-6 pyridine) copolymers P($TP_{x\%}$-co-$CE_{y\%}$) via a facile superacid-catalyzed Friedel-Crafts reaction. Owing to pyridine/crown ether units and microphase separation, the P($TP_{91\%}$-co-$CE_{9\%}$) membrane showed a 205% PA doping level and 0.138 S cm^{-1} conductivity at 180 °C. The corresponding H_2-O_2 cell delivered a peak power density of nearly 1200 mW cm^{-2} under non-humidified and non-backpressure conditions, showing great potential for high-performance HT-PEMFCs [41]. They also fabricated a series of imidazole-containing conjugated copolymers P($BF_{x\%}$-$TP_{y\%}$-Im) via a simple polymerization route, as illustrated in Figure 4a. Benefiting from imidazole units and dibenzofuran-derived structures, the copolymer membrane showed efficient PA doping and proton conduction. As shown in Figure 4 b–d, the optimized membrane exhibited peak power densities of 1085 and 539 mW cm^{-2} in H_2–O_2 and H_2–air fuel cells at 180 °C, and exhibited outstanding long-term stability with a low voltage decay rate of 4.3 μV h^{-1} over 720 h [42].

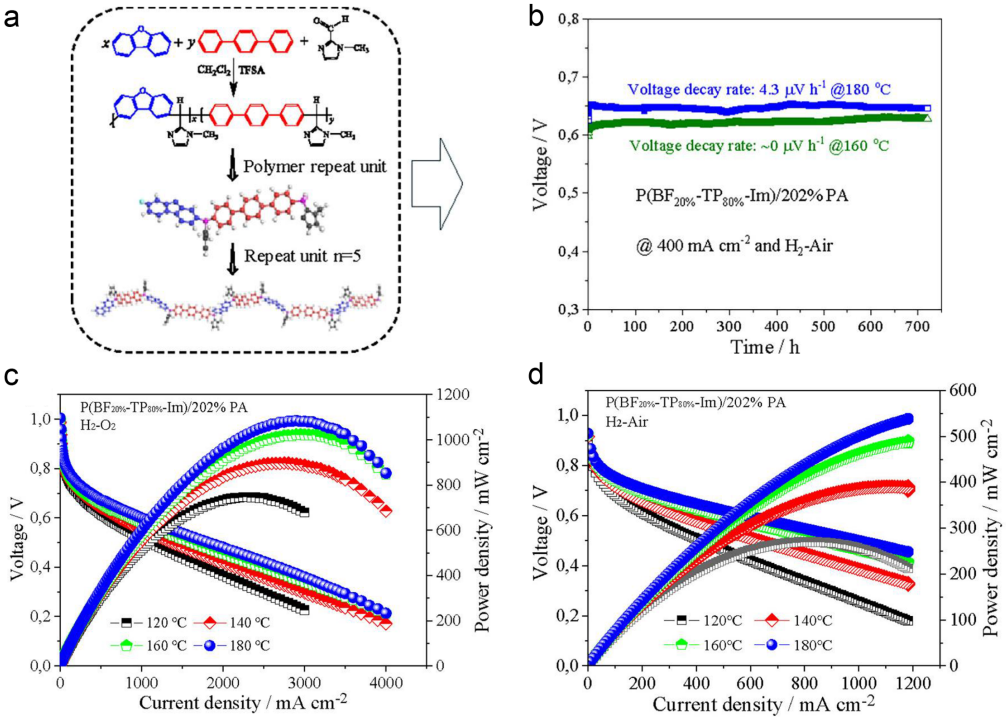

Figure 4. (**a**) Synthesis of P($BF_{x\%}$-$TP_{y\%}$-Im) copolymers; (**b**) durability of the H_2–air cell with P($BF_{20\%}$-$TP_{80\%}$-Im)/202%PA under 400 mA cm^{-2} at 160 and 180 °C; P($BF_{20\%}$-$TP_{80\%}$-Im)/202%PA operating with H_2–O_2 (**c**), and H_2−air (**d**) under ambient pressure [42], Copyright 2025, American Chemical Society.

In recent studies, quaternary ammonium (QA) polymers have been investigated as high-temperature proton exchange membranes to improve phosphoric acid retention. QA hydroxides exhibit relatively strong alkalinity, enabling complete deprotonation of PA to form strong QA^+-$H_2PO_4^-$ ion pairs, which interact much more strongly than the interaction between PA and water. This effectively prevents PA loss caused by water. Lee et al. [43]

proposed a class of polyphenylene-based high-temperature proton exchange membranes based on QA-biphosphate ion-pair-coordinate (PA-doped QAPOH). The assembled fuel cells demonstrated stable performance at temperatures ranging from 80 to 160 °C. After 44 h of testing under conditions of 80 °C and 40% RH, the PA retention rate remained as high as 93%. Moreover, the rate of through-plane proton conductivity decay at 80 °C and 150 mA cm^{-2} was more than three orders of magnitude lower than that of PA/PBI membranes. Under 120 °C H_2/air for 500 h, the QAPOH MEA shows no performance degradation. In accelerated thermal cycling (80–160 °C), the PA/PBI MEA fails within 70 cycles, while QAPOH exhibits stable performance with a voltage decay of −0.39 mV/cycle at 160 °C and retains 60% of its PA doping after 500 cycles.

Chen et al. [44] prepared the long alkyl side chains with quaternary ammonium groups grafted polybenzimidazole membranes (PBI-Sc-X). Due to the strong ion-pair interaction between quaternary ammonium groups and biphosphate, the PA doping level and PA retention were remarkably improved, Compared to PBI, PBI-Sc-35 exhibited an increase in proton conductivity from 65 mS cm^{-1} to 104 mS cm^{-1} at 170 °C. After operating for 12 h at 150 °C, the retention rate of proton conductivity for PBI-Sc-35 remained 80%, while PBI only maintains about 60%. Besides, PBI-Sc-5 membrane held the highest power density of 411.7 mW cm^{-2} at 160 °C and 1000 mA cm^{-2}.

In a parallel pursuit, Jiang et al. [30] employed a copolymer, QPAF-4, featuring quaternary ammonium group modification at the terminal end of the side chain for the high-temperature proton exchange membrane. Due to the intrinsic micro-phase separation structure of QPAF-4 matrix and strong interaction of QA and PA, the PA-doped membranes possessed high proton conductivity and eminent PA retention. Notably, the QPAF-4-150%PA membrane achieved a maximum power density of 683 mW cm^{-2} at 160 °C under anhydrous condition. Furthermore, the corresponding single fuel cell shows excellent stability, operating steadily for more than 60 h at 140 °C.

2.2. Polymers with High Free Volume

For high-temperature proton exchange membranes using PA as proton carrier, acid doping level is a key determinant of membrane conductivity. Increasing the free volume within the membrane is an effective strategy to enhance the adsorption and retention of phosphoric acid molecules [45–47]. This can be accomplished by incorporating rigid or voluminous groups to mitigate the tight packing of molecular chains. Branched polymers with distinctive three-dimensional dendritic structure afford the membrane with accessible and interconnected cavities, these cavities function to increase the free volume within the membrane.

Polymers of intrinsic microporosity (PIMs) are characterized by abundance of twisted rigid sites in main-chain structure, resulting in the formation of inherent micropores (pore size < 2 nm). Tang and Geng [31], presented PA-doped intrinsically ultra-microporous membranes constructed from rigid, high free volume, Tröger's base-derived polymers. Membranes with an average ultramicropore radius of 3.3 Å showed a siphoning effect with phosphoric acid molecules, and upheld a high PA retention rate even under conditions of elevated humidity. The proton conductivity retention rate surpassed that of PA/PBI membranes by more than three orders of magnitude. Remarkably, DMBP-TB/PA boasted a peak power density of 815 mW cm^{-2} at 160 °C, which was twice that of *m*-PBI/PA. Moreover, the substantially advanced properties of DMBP-TB/PA enabled the MEA to operate within a broad temperature range from –20 °C to 200 °C. DMBP-TB/PA MEAs showed exceptional stability in low-temperature accelerated stress tests (AST), enduring over 150 cycles at 40 °C and 15 °C and retaining 95% peak power density and 86% ADL after 150 cycles at 15 °C, while *m*-PBI/PA MEAs fail after only 2 cycles at 40 °C, and high-temperature durability is not evaluated in this work.

Compared with linear polymers, the microstructure formed by branched polymers endows a larger free volume to accommodate more PA molecules without sacrificing dimensional stability, rendering them propitious for PA retention. Wang et al. [32] synthesized PBIs with different degree of branching, where the branched PBI exhibited higher ADL and proton conductivity. Among them, the membrane with the highest degree of branching, OPBIR2-9, showed the highest proton conductivity (53 mS cm^{-1} at 180 °C) and the best antioxidant stability. Additionally, the peak power density of OPBI-R2-9 (222 mW cm^{-2}) was almost double that of linear OPBI (125 mW cm^{-2}) at 160 °C under anhydrous conditions. However, the higher degree of branching resulted in inferior mechanical properties of the branched PBI.

Wang's group [48] designed a series of highly branched PBIs with 1,3,5-tri(4-carboxyphenoxy)benzene as a branching agent. The ADL for the branched polybenzimidazole with a 9% degree of branching characterized an ADL of 10.5, which was notably higher than that of *p*-PBI (4.6) and OPBI (5.6). Wang et al. [33] also reported a branched PBI core block with another derived PBI structure, the starshaped polymer backbone provided dual advantages of increased free volume and microscopic phase separation, endowing the membranes with high PA doping capacity and efficient proton transport. The ADL of Br*p*PBI-*b*-F6-PBI reached 17.5, achieving a high proton conductivity of 150 mS cm^{-1} and a power density of 713 mW cm^{-2} at 160 °C without humidification.

2.3. Cross-Linked Polymers

Cross-linking entails the covalent bonding of linear or branched polymer chains, leading to the formation of a network or bulk polymer structure. Compared with linear and branched structure polymers, cross-linked polymers exhibit higher hardness and brittleness, which could reduce the substantial softening of PA-doped membranes. At comparable or even higher levels of phosphoric acid doping, crosslinked membranes can sustain reduced dimensional swelling, thus enhancing membrane mechanical properties without compromising proton conductivity [49–52]. Crosslinking structures are also widely recognized for their ability to restrict the loss of phosphoric acid [53–56].

Hu et al. [34] synthesized a series of cross-linked polybenzimidazole membranes by using a hyperbranched cross-linker with quaternary ammonium. The resulting QOPBI-15 manifested an elevated tensile strength of 27.0 MPa, greatly surpassing the value of 18.5 MPa exhibited by PBI. The introduction of rigid networks compressed the molecular chains and reduced the uptake of PA, yet the proton conductivity remained unaffected due to the incorporation of QA groups.

Based on the branched F6PBI, Wang et al. [35] prepared crosslinked membrane using polybis(3-phenyl-3,4-dihydro-2H-1,3-benzoxazinyl) (*p*(BA-a)) as a macromolecular crosslinker. The increase in free volume and phosphoric acid adsorption capacity led to an enhancement in proton conductivity of the membrane. The mechanical properties and antioxidant stability of these membrane had been simultaneously improved along with the crosslinking. The H_2/O_2 fuel cell assembled with C10F6-R2-6 membrane reached a peak power density of 690 mW cm^{-2} at 160 °C. At 160 °C and 200 mA cm^{-2}, the PA-doped C10F6-R2-6 membrane-based single cell exhibited stable OCV and low internal resistance over a 200h durability test. The cell maintained a high and nearly constant voltage, demonstrating excellent stability and proton conductivity for high-temperature PEMFC operation.

As shown in Figure 5a, in a recent work of Wang et al. [36], a locally high-density cross-linked network of PBI was synthesized using pillar[5]arene featuring multiple alkyl bromide moieties, and the residual unreacted halides were transformed into ammonium salts to introduce additional acidophilic sites for PA absorption and proton transportation. As illustrated in Figure 5b,c, the locally concentrated distribution of cross-linking sites, coupled with loosely packed PBI segments between adjacent cross-linkers, facilitated the increased retention of PA molecules within the cross-linked network. The OPBI-CL-Pillar-7% membrane characterized by a high gel content of 90.7% demonstrated a noteworthy conductivity of 116.8 mS cm^{-1} at 160 °C alongside excellent mechanical strength, measuring at 14 MPa. Besides, it exhibited a remarkable power density of 1084 mW cm^{-2} at 180 °C. OPBI-CL-Pillar-7% membrane exhibits a low voltage decay rate of 0.0395 mV h^{-1} during 200 h fuel cell testing at 160 °C and 200 mA cm^{-2}, superior to other PA-PBI membranes.

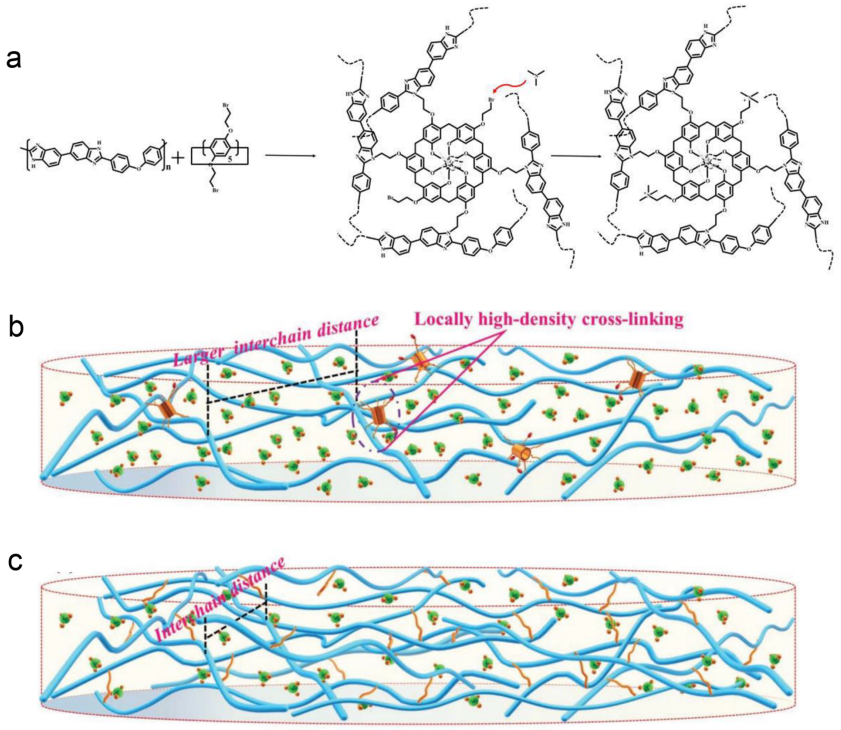

Figure 5. (**a**) Chemical reactions associated with pillar[5]arene-cross-linked network. Molecular structures and feature of (**b**) pillar[5]arene-based and (**c**) conventional cross-linked network [36], Copyright 2022, John Wiley and Sons.

2.4. Phosphonated Polymers

Phosphonated polymers have been a focus of researchers' efforts, as the covalent immobilization of acid groups ensure no leakage even in the presence of water vapor or even liquid water. However, due to the restrictions of lower dissociation constant and ion mobility, their proton conductivity tends to be lower and shows a reliance on water, making 'free' phosphonic acids indispensable [57–59]. Moreover, phosphonated polymers suffer from mechanical fragility at high ion exchange capacity (IEC), thereby constraining their application. Kerres research group[60] grafted poly(pentafluorostyrene) (PFS) on a preirradiated ethylene-tetra-fluoro-ethylene (ETFE) film, followed by a post-phosphonation or post-sulfonation of the PFS grafting chains. The PFS grafted ETFE with phosphonation and sulfonation degree of 50% and 70% (IEC = 1 and 1.5 mequiv g^{-1}) exhibited conductivities of 90 and 170 mS cm^{-1} at 120 °C and 90% RH, respectively. Abouzari-Lotf et al. [61] synthesized highly phosphonated copolyimide ionomers with IEC of 2.4∼4.6 mequiv g^{-1}, a proton conductivity value of only 2.5 mS cm^{-1} was measured in dry condition at 120 °C, which was 2–3 order of magnitude lower than in saturated water), showed a high dependence on humidity.

Song and Li et al. [62] demonstrated the synthesis of polysiloxanes grafted with both tetrazole and phosphonic acid groups, the prepared membranes were then doped with free PA. Protons can be efficiently transferred between adjacent nitrogen atoms, grafted acid groups, and free phosphoric acid. The membrane achieved ~190 mW cm^{-2} at low free PA doping (5.2 wt.%) and low humidity (120 °C, 1.2% RH). The conductivity and cell performance at elevated temperatures were not studied here, but it shows the advantages of reasonable structural designation of phosphonated polymers, and also, their development converges on a synergy with free phosphoric acid. In a recent work, Hao et al. [37] investigated bifunctional poly (p-terphenyl-co-isatin piperidinium) (P/PTIP-x) copolymer with tethered phosphonic acid and tertiary amine base groups as HT-PEMs, with low PA uptake (<100%), the copolymers displayed a conductivity of 99 mS cm^{-1} and a peak power density of 812 mW cm^{-2} at 160 °C. At 140 °C, the 70%PA@P/PTIP-40 membrane displays a much lower voltage degradation rate of 0.08 mV h^{-1} over 100 h at 150 mA cm^{-2}, compared with 0.45 mV h^{-1} for 90%PA@P/PTIP-20. It also exhibits higher voltage and peak power density retention, resulting from stronger hydrogen-bond interactions and higher PA retention.

3. Composite Membranes

In recent years, there have been significant advancements in the development of composite HT-PEMs. Composite membranes obtained through blending or doping with two or more materials synergize the merits of individual components to collectively enhance the overall performance. Additionally, targeted modifications effectively address various challenges in PEM applications.

3.1. Organic-Organic Composite Membranes

Organic-organic hybridization involves combining alkaline polymers with organic components featuring specific structures or unique properties, such as acid-functionalized polymers, hydrophobic polymers, polymers of intrinsic microporosity, ionic liquids, porous organic networks, etc. The incorporation of these organic components not only strengthens the mechanical properties of the hybrid electrolyte membrane, but also plays a role in the distribution of PA and the facilitation of protonic conduction [63–68]. Table 2 provides a summary of some representative organic-organic composite membranes and the corresponding key performance parameters.

The blending of polymers is an efficacious method to elevate the singular polymer material's strength, toughness, and thermal resilience. Acid-functioned polymers, exemplified by sulfonated polymers and phosphonated polymers, engage in interactions with basic polymer matrix, contributing to the formation of acid-base composite membranes—as called ionic crosslinked membranes. Due to the enhancement of intermolecular forces, ionic crosslinking can effectively improve the mechanical properties and antioxidant stabilities of PBI-based high-temperature proton exchange membranes [69–71]. Furthermore, Suzuki et al. [72] reported that PA-doped sulfonated polyimide (SPI) and PBI composite membranes formed a new proton transport pathway between $H_3PO_4/H_2PO_4^-$ and SO^{3-}, and protons could be efficiently transported under conditions of low humidity and even anhydrous state. Liu et al. [73] also unveiled the additional proton transport channels within the phosphoric acid-doped poly(arylethersulfone) (SPAES) and polybenzimidazole (PBI) composite membranes. Bai et al. [69] incorporated sulfonated poly (fluorenyl ether ketone) (SPFEK) into the OPBI membrane, resulting in composite membranes with notably enhanced mechanical properties. OPBI-SPFEK 10% with 216% PA uptake demonstrated a tensile strength of 24.7 MPa and achieved a maximum power density of 727 mW cm^{-2} at 160 °C, marking a 26% and 21% increase over pristine OPBI, respectively. As illustrated in Figure 6, Hao et al. [74] proposed partially replacing free PA with immobilized PA based on phosphonated phenol-formaldehyde (PPF) to construct long-

range proton transport channels in the PPF/PBI composite membranes. 50PPF/PBI membrane with PA uptake of 165% reached a peak power density of 607 mW cm^{-2} at 160 °C. At 140 °C and 125 mA cm^{-2} for 50 h, the 50PPF/PBI MEA shows a voltage attenuation rate of only 12%, demonstrating excellent durability owing to its superior PA retention.

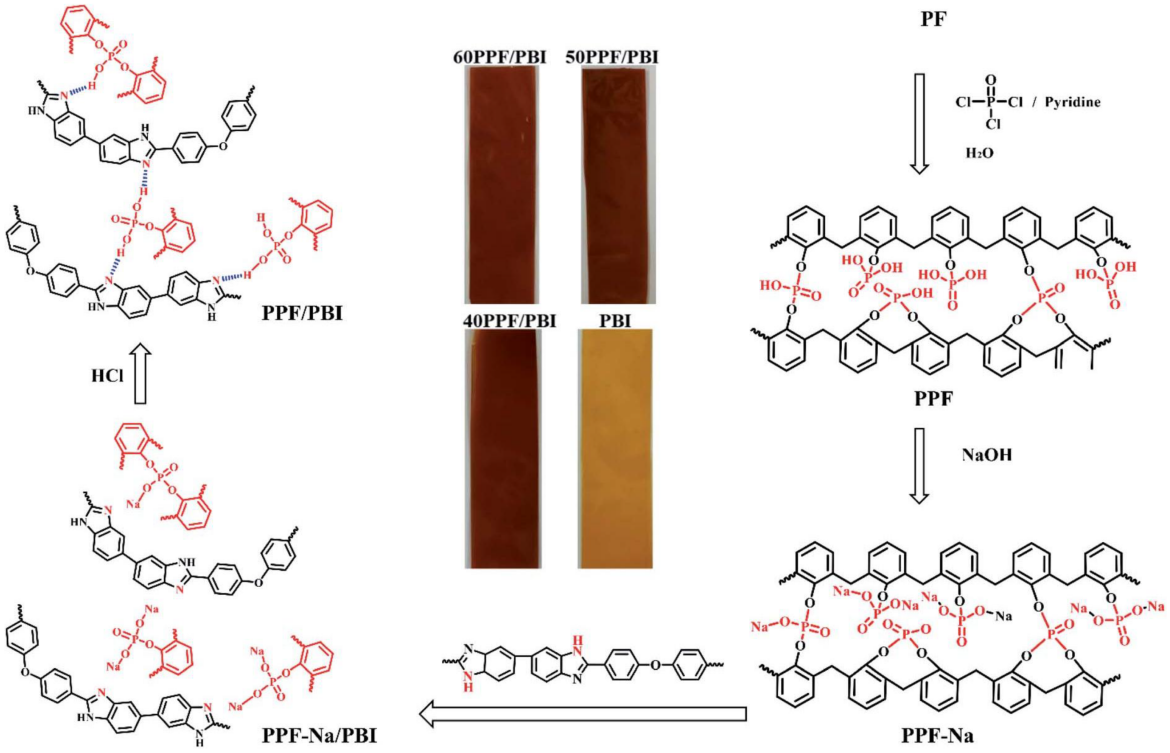

Figure 6. The synthetic route to the PPF/PBI membrane [74], Copyright 2022, Royal Society of Chemistry.

Table 2. Key performance parameters of some organic-organic and organic-inorganic composite high-temperature proton exchange membranes.

Membrane	Filler	Inorganic Content (wt.%)	PA Uptake (%)	Proton Conductivity (mS cm^{-1})	Fracture Stress (MPa)	Peak Power Density (mW cm^{-2})
50PPF/PBI [74]	/	/	165	62 (140 °C)	13.1	607
OPBI-SPFEK 10% [69]	/	/	216	50	24.7	727
PVDF-PVP80 [75]	/	/	~250	67 (150 °C)	~2.0	530 (180 °C)
6FPBI-cPIL 20 [76]	/	/	ADL = 27.8	106 (170 °C)	2.9	/
OPBI/L-10 [77]	/	/	ADL = 18.7	257	8.9	438
PBI/30%-SNW-1 [78]	/	/	175	114	~4.0	590
30%-CTFs-OPBI [79]	/	/	167	71	7.7	534
PBI/SNP-PBI-10 [80]	PBI-SiO_2	10	385	50 (160 °C)	/	650 (150 °C)
PBI-sTP2 [81]	s-TiO_2	2	386	96 (150 °C)	/	621 (150 °C)
Py-PBI/1.5%PGO [82]	PGO	1.5	ADL = 9.9	76 (140 °C)	4.65	359 (120 °C)
rGO-PBI-1 [83]	reduced GO	1	ADL = 8.9	126 (170 °C)	/	743 (170 °C)
PBI/MWCNT-Nafion [84]	MWCNT–Nafion	0.2	ADL ≈ 11.5	50 (160 °C)	/	700 (150 °C)
PBI/1Mus [85]	muscovite	1	434	42 (150 °C)	7.5	586 (150 °C)
ABPBI/α-ZrP [86]	α-ZrP	10	ADL = 6.5	46 (180 °C)	36.0	400 (160 °C)
PSC_8 [87]	$SrCeO_3$	8	190	105 (180 °C)	/	~700 (180 °C)
SPAEK-SPOSS-1% [88]	SPOSS	1	193.2	126 (200 °C)	18.7	300
PBI@ ZIF-mix [89]	ZIF-mix	5	157	91 (200 °C)	/	/
40%UIO-66@OPBI [90]	UIO-66	40	73	92 (160 °C)	27.02	583

* H_2/O_2 fuel cell performances (160 °C).

Mixing hydrophobic polymers without acidic functional groups with PBI can provide mechanical strength to the substrate, thereby enhancing the level of phosphoric acid doping or enabling the preparation of thinner membranes, thus improving the overall efficiency of fuel cells. Jana et al. [91] elucidated that blending PBI polymer with polyvinylidene fluoride (PVDF) in a certain proportion substantially increased the phosphoric acid doping level of the membrane. Polyvinylpyrrolidone (PVP), characterized by basic nitrogen heterocycles yet water-soluble, cannot independently serve as high-temperature proton exchange membranes, researchers blended PVP with other polymers, such as polyether sulfone (PES) and PVDF, to enhance the mechanical strength [75,92,93].

Jiang et al. reported that the 20 wt.% PVDF–80 wt.% PVP membrane (H_3PO_4 doping level 2.7) achieved a proton conductivity of 0.093 S cm^{-1} at 200 °C under anhydrous conditions, comparable to state-of-the-art PBI/PA membranes; its PA-doped PVDF–PVP80 membrane exhibited high power density (530 mW cm^{-2} at 180 °C in H_2/O_2), negligible current decay over 240 h at 150/160 °C under 0.5 V, and no PA leaching for 10 days [75].

From another perspective, Wang et al. [77] incorporated polymers of intrinsic microporosity into OPBI matrix, the authors contended the addition of PIMs can bring a large free volume into the alloy membranes, which enhanced the ADLs and proton conductivity. A notable proton conductivity of 313 mS cm^{-1} was attained at an operating temperature of 200 °C, accompanied by a peak power density reaching 438 mW cm^{-2} at 160 °C.

In addition to the aforementioned polymer blends, some organic small molecules, and emerging porous organic networks, have also been employed in blends with PBI and other polymer materials. Some attempts with organic fillers proved suboptimal, for instance, Schecheter and Savinell [94] observed that the inclusion of imidazole (IM) or 1-amyl imidazole (Me-IM) in PA/PBI membranes resulted in a decrease in proton conductivity, attributed to imidazole's binding to free phosphoric acid, thereby reducing the concentration of proton charge carriers.

Ionic liquids (ILs) refer to organic salt comprising organic cations and inorganic/ organic anions. They are liquid at room temperature, exhibiting high thermal stability and possess a wide electrochemical window, making them suitable for use as a proton conductor [95–97]. ILs have been utilized in the fabrication of HT-PEMs and MEAs. However, their performance is often unsatisfactory. To fulfill the demands for proton conduction, ILs are frequently loaded at excessively high levels, posing significant obstacles to electrode catalyst efficiency and leading to considerable IL leakage concerns. Some recent work replaced ILs with polyprotic ILs (PILs), e.g., Liu et al. [76] mixed PIL containing imidazole to provide continuous pathways for proton transport in 6FPBI, and introduced a cross-linked structure through the hydrolysis of KH-560. The proton conductivity of the resulting composite membrane was 106 mS cm^{-1} at 170 °C, nearly double that of 6FPBI, while the assessments of fuel cell performance were absent.

Porous organic networks are newly emerged filler materials for polyelectrolytes in energy conversion field. Our group [78] synthesized a Schiff-base type porous polymeric network (SNW-1) with abundant N–H sites and blended with OPBI. At a doping level of 30%, the PA uptake of PBI/30%-SNW-1 membrane decreased to 175.0%, while the proton conductivity significantly increased to 114.0 mS cm^{-1} at 160 °C. The pristine PBI had a PA uptake of 270.0% and a proton conductivity of 67.3 mS cm^{-1}, respectively. The peak power density of the PBI/30%-SNW-1 composite membrane reached 590 mW cm^{-2} at 140 °C, higher than that of PBI at 450 mW cm^{-2}. Additionally, the PBI/30%-SNW-1 composite membrane showed enhanced proton conduction stability, which experienced only an 8.47% decline in proton conductivity after a 30-h evaluation at 140 °C, compared to 12.84% for pristine PBI. Peng et al. [79] conducted in-situ synthesis of covalent triazine-based frameworks (CTFs) within polybenzimidazole under mild trifluoromethanesulfonic acid (TFA) catalysis. The membrane containing 30% CTFs exhibited high conductivity of 74.8 mS cm^{-1} under low PA doping level of 167.1%. The peak power density of the single cell assembled with the 30%-CTFs-OPBI composite membrane reached 534.4 mW cm^{-2}, significantly suppressed that of OPBI under the same phosphoric acid doping level and testing conditions (325.2 mW cm^{-2}), which was also higher than that of directly blended B30%-CTFs-OPBI. This indicates that constructing stable continuous proton transport channels can achieve efficient proton conduction at relatively low levels of phosphoric acid doping. At 160 °C and 200 mA cm^{-2} for 250 h, the 30%-CTFs-OPBI membrane exhibits stable voltage, showing low H_2 permeability and high stability.

3.2. Organic-Inorganic Composite Membranes

Inorganic nanofillers always demonstrate robust rigidity, their incorporation into HT-PEMs is promising to augmenting the mechanical-dimensional stability of composite membrane. An inorganic component may also assist in improving the thermal stability, acid retention, reactant crossover resistance, conductivity and other properties of the polymer membranes [98–101]. A host of inorganic materials have been used for preparation of nanocomposite membranes, some representative examples are summarized in Table 2, they can be classified into the following five categories: (I) hygroscopic metal oxides, such as SiO_2, TiO_2, ZrO_2, etc.; (II) active carbon materials, such as graphene oxide, carbon nanotubes, etc.; (III) nanoclays; (IV) proton conductor, such as metal phosphates, acceptor-doped perovskite-type oxides, polyhedral oligomeric silsesquioxane (POSS), etc.; (V) metal organic frameworks (MOFs).

Functional hygroscopic metal oxides demonstrate the capability to trap phosphoric acid in the corresponding composite membranes, thereby increasing the proton conductivity of the membranes. Suryani et al. [80] synthesized PBI-functionalized silica nanoparticles (SNPs) for incorporation into PBI composite membranes. The PBI/SNP-PBI composite membrane containing 10 wt.% SNP-PBI demonstrated a 25% higher conductivity than pristine PBI

at 160 °C. Moreover, the PBI/SNP-PBI membrane exhibited a maximum power density of 650 mW cm^{-2}, surpassing the 530 mW cm^{-2} value of the pristine PBI membrane. Lee et al. [81] synthesized sulfonated TiO_2 nanoparticles (s-TiO_2) as a filler for *m*-PBI, and the composite membrane containing 2 wt.% s-TiO_2 obtained up to an ADL of 12.1 and a peak power density of 621 mW cm^{-2} at 150 °C, an ascent of 30% over pure PBI membrane.

Graphene oxide (GO) possesses a substantial specific surface area, excellent mechanical properties, and abundant hydrophilic oxygen-containing groups, which endow it with the ability to conduct protons and enhance mechanical strength. Abouzari-Lotf et al. [82] used phosphonated graphene oxide (PGO) as the filler of 2,6-Pyridine functionalized polybenzimidazole (Py-PBI), which notably improved the tensile strength, proton conductivity and single cell power density of Py-PBI. The Py-PBI/1.5% PGO membranes (ADL = 9.93) exhibited a proton conductivity of 76.4 mS cm^{-1} at 140 °C and maximum power density of 359 mW cm^{-2} at 120 °C. The retention rate of proton conductivity was also significantly improved. Ko et al. [102] employed GO and poly(2,5-benzimidazole)-grafted graphene oxide (ABPBI-GO) as fillers for sulfonated poly(arylene ether sulfone) (SPAES) composite membranes. SPAES/ABPBI-GO demonstrated enhanced dimensional stability, increased Young's modulus, and elongation at break values compared to SPAES/GO, attributed to acid-base interactions. Besides, the SPAES/ABPBI-GO composite membranes exhibited superior conductivity relative to both pristine SPAES and SPAES/GO composite membranes. Ghosh et al. [83] reported PBI composite membranes with reduced GO (rGO). The optimum loading of 1wt.% rGO improved the value of proton conductivity up to 126 mS cm^{-1} and generated a higher maximum power density at 170 °C, reaching 743 mW cm^{-2}, approximately twice that of the pristine PBI (368 mW cm^{-2}). rGO-PBI-1 also exhibited the highest tensile strain, phosphoric acid retention rate, and chemical stability.

Suryani et al. [84] synthesized Nafion- and PBI-functionalized multiwalled carbon nanotubes (MWCNT-Nafion and MWCNT-PBI) as additives in composite membranes. The addition of functionalized MWCNTs enhanced the mechanical properties of PA-undoped membranes. The PA-doped nanocomposite membranes containing 0.2 wt.% of MWCNT–Nafion (N-0.2) and MWCNT–PBI (P-0.2) demonstrated conductivities of 0.05 S cm^{-1} and 0.08 S cm^{-1} at 160 °C, maximum power densities of 700 mW cm^{-2} and 600 mW cm^{-2} at 150 °C, which were superior to the pristine PBI membrane (530 mW cm^{-2}).

The incorporation of clay minerals into membranes has attracted interests because of their hygroscopicity, high surface area and low cost. Clay–based materials such as montmorillonite [103], sepiolite [104,105], and vermiculite [106] were explored as the membrane additives in HT–PEMFC applications. In a work of Guo et al. [85], muscovite (Mus) was incorporated into PBI matrix as an inorganic filler. The membrane with 1 wt.% Mus showed the highest mechanical strength and lowest dimensional swelling, and the highest power density of 586 mW cm^{-2} at 150 °C without humidification, which was 24% higher than the pure PBI membrane (474 mW cm^{-2}). Under accelerated stress testing (AST), the composite membrane exhibited significantly enhanced durability, because the Mus–PA crosslinks could improve the acid retention ability of PBI/Mus composite membranes to alleviate catalyst degradation. Compared with the pristine PBI membrane, the composite membranes exhibited significantly enhanced durability under accelerated stress test (AST). Among them, PA/PBI/2Mus shows the lowest voltage decay rates (0.226 mV h^{-1} at OCV, 1.042 mV h^{-1} at 0.6 A cm^{-2}, 1.298 mV h^{-1} at 1.0 A cm^{-2}), much lower than the pure PBI membrane, owing to effectively suppressed PA leaching.

Metal phosphates, such as zirconium phosphates (ZrP) and boron phosphates, can provide additional proton conduction pathways for PEM, besides the potential reinforcement effects. Rao et al. [86] reported the fabrication of nanocomposite membranes based on ABPBI/α-ZrP. The composite membrane containing 10 wt.% hydrophilic α-ZrP showed an increase in ADL from 3.6 to 6.5 compared to the original ABPBI membrane, with the proton conductivity at 180 °C increasing from 27 mS cm^{-1} to 46 mS cm^{-1}. The proton transport pathways in the composite membrane are depicted in Figure 7a. More remarkably, the thermo-mechanical properties and oxidative stability were improved simultaneously. Stress-strain profiles of the undoped and doped membranes are shown in Figure 7b,c. The nanocomposite membrane with 10 wt.% of α-ZrP showed an excellent tensile strength of 36.0 MPa, besides, the single-cell showed a peak power density of about 400 mW cm^{-2} at 160 °C. Under start-up/shut-down mode at 200 mA cm^{-2}, the 100 W stack delivered stable voltage with a decay rate of 0.84 μV h^{-1} over 730 h. Acceptor-doped perovskite-type oxides are also recognized as high-temperature proton conductors, holding promise for applications in devices like fuel cells. In a work of Shabanikia et al. [87], perovskite-type $SrCeO_3$ nanoparticles were used for improving the properties of PBI membranes. Improved PA uptake and proton conductivity were observed in the composite membranes. By incorporating 8wt.% $SrCeO_3$ into the composite membrane, PSC_8 exhibited the highest phosphoric acid uptake at 190% and conductivity of 0.105 S cm^{-1} at 180 °C. During fuel cell testing, it achieved a power density of 440 mW cm^{-2} at 0.5 V. Yang et al. [88] incorporated polyhedral-oligosilsesquioxane nanoparticles bearing sulfuric acid groups (SPOSS) into a phenylated arylether-type PBI (Ph-PBI), these hybrid membranes exhibited enhanced ADLs, acid retention ability and attractive mechanical-

dimensional stability. The proton conductivity of SPAEK-SPOSS-1% with 193% PA reached 126 mS cm^{-1} at 200 °C, and a peak power density of 300 mW cm^{-2} at 160 °C. Especially, the membrane exhibited a tensile strength of up to 18.7 MPa.

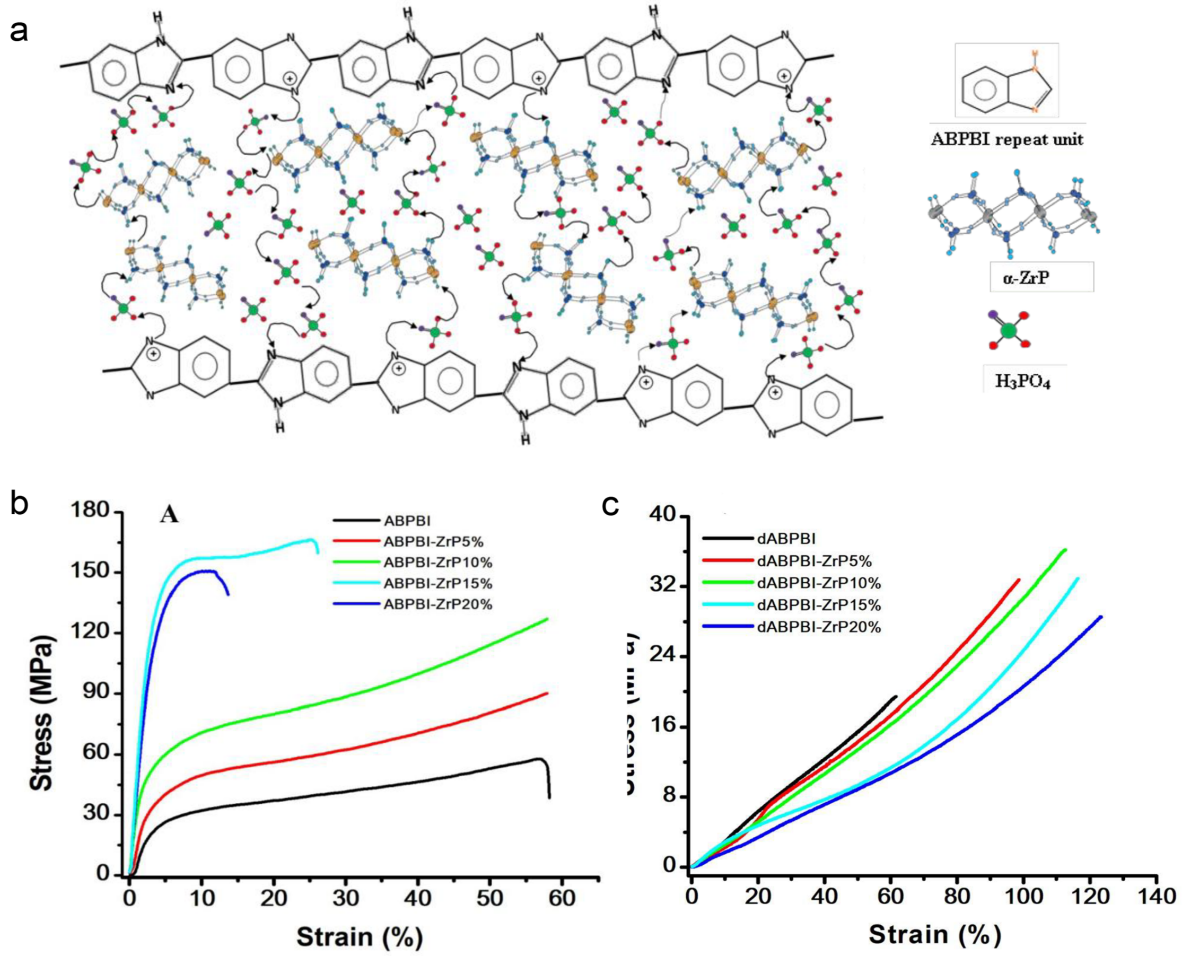

Figure 7. (**a**) Schematic of proton conducting channels in PA-doped ABPBI-α-ZrP nanocomposite membrane. Stress-strain profiles of (**b**) undoped and (**c**) doped ABPBI membranes as a function of α-ZrP loading [86], Copyright 2019, American Chemical Society.

Metal-organic frameworks (MOFs) possess qualities of high specific surface area, substantial porosity, and high designability. In recent years, MOFs have attracted contemporary explorations in field of high-temperature proton exchange membranes. Escorihuela et al. [89] incorporated zeolitic imidazolate framework, including ZIF-8, ZIF-67, and their binary mixture, to build a series of PBI composite membranes. The proton conductivities of these membranes were higher than that of pure PBI and pure ZIFs. PBI@ZIF-8, PBI@ZIF-67 and PBI@ZIF-mix composite membranes containing 5 wt.% ZIFs exhibited proton conductivities of 3.1 mS cm^{-1}, 41 mS cm^{-1}, and 92 mS cm^{-1} at 200 °C and anhydrous conditions, respectively. Chen et al. [90] infused a Zr-based metal-organic framework (UIO-66) into the OPBI matrix, the composite membranes exhibited long-range continuous proton transport channels, which endowed a conductivity of 92 mS cm^{-1} at a PA uptake of only 73%. At 160 °C and 200 mA cm^{-2} for 500 h, the 40%UIO-66@OPBI membrane exhibits a voltage decay rate of 0.15 mV h^{-1}. After 12 restart cycles up to 160 °C, it maintains a peak power density of 500 mW cm^{-2} with stable resistance, whereas the 0%UIO-66@OPBI membrane shows decreased power and increased resistance.

3.3. Nanofiber Reinforced Membranes

Recently, electrospun polymer nanofibers have gained prominence in energy applications [107–109]. The flexible and porous nanofiber mat offers a three-dimensional support for polymer electrolyte membranes [110–113]. In contrast to inorganic nanoparticles, nanofibers easily and naturally weave themselves into the PEM matrix, their three-dimensional structure can effectively constrain the deformation issues of phosphoric acid-doped membranes, enhancing the mechanical properties of the membrane.

Li et al. [114] utilized a polytetrafluoroethylene (PTFE) porous membrane as the substrate to prepare a PTFE/PBI composite membrane. The PTFE matrix provided excellent mechanical properties, after doped with phosphoric acid, the composite membrane also showed good proton conductivity and relatively stable durability. At 150 °C and 0.7 A cm^{-2} for 50 h under atmospheric air, the PTFE/PBI/H_3PO_4 composite membrane shows only a slight performance decay, demonstrating good interim stability. Lu et al. [115] synthesized PTFE porous membrane reinforced PVP-PES composite membrane, which significantly enhanced the tensile strength and Young's modulus of the PA-doped membranes. The PES–PVP/PTFE composite membranes with optimized impregnating degree exhibited a proton conductivity of 0.26 S cm^{-1} and a maximum power density of 607 mW cm^{-2} at 180 °C.

Our research group have explored polypyrrolone (PPy) as the polymeric material for HT-PEMs [116], the composite membrane comprised of PPy-impregnated polyimide nanofiber mat (PI@PPy) demonstrated improved dimensional stability, with notable reduction in PA swelling ratio, which was 51% in area and 25% in volume. PI@PPy exhibited 62% higher yield strength, superior peak power density of 634 mW cm^{-2} at 160 °C, and less cell voltage reduction in durability tests, highlighting the trade-off between proton conductivity and PA retention ability.

Nanofibers modified with specific functional groups can interact better with polymer electrolytes to effectively improve the performance of PEM. in a work of Lu et al. [117], carbon fiber (CF) were oxidized and reduced to introduce hydroxyl, carboxyl and amino groups, allowing the in situ polymerization of PBI on the surface of the CF. The flexural strength and tensile strength of the resultant CF/PBI composite membranes were significantly improved.

3.4. Multi-Layer Structure

Constructing spongy porous HT-PEM is an effective strategy to increase the ADL, however, porous structures cause cross penetration of fuel gas, PA leakage, and low mechanical strength. A promising solution is covering both sides of a porous membrane with a dense skin layer, yet the preparation of the three-layer membrane has always been a problem.

Cai et al. [118] synthesized sulfonated graphene oxide (RGO) with high ion exchange capacity and coated porous PBI membrane with PBI-RGO on both sides via the layer-by-layer method. The phosphoric acid doping level of multilayer membranes increased with the mass fraction of porous PPBI layers. PBI-RGO/PPBI-80/PBI-RGO adsorbed 500 wt.% of phosphoric acid, achieving a proton conductivity of 0.113 S cm^{-1} at 170 °C under non-humidified conditions, with a high tensile strength of 22.7 MPa. After testing at 180 °C for up to 10,000 h, the three-layered membrane cells show much lower voltage decay rates (2.3 and 4.1 mV h^{-1}) than single-layered ones (14 and 11 mV h^{-1}).

Wang et al. [119] developed a novel membrane-making process for the preparation of asymmetric three-layer membrane, its structure is shown in Figure 8a. The thin skin layer and porous layer were prepared by using the nonsolvent induced phase separation (NIPS) method on the preprepared thick skin layer. A high level of PA doping was achieved due to this structure, and the as-prepared three-layer HT-PEM exhibited a peak power density of 713 mW cm^{-2}. Furthermore, the durability of the three-layer HT-PEM fuel cell was significantly enhanced by introducing a cross-linking agent KH-560, with only 0.064 mV h^{-1} load voltage decay observed after 200 h, as shown in Figure 8b.

Li et al. [120] prepared dense double skin layers on porous PBI membrane by crosslinking with amino tris (methylene phosphonic acid) (ATMP), as depicted in Figure 8c. As a proton conductor, ATMP also participated in the formation of hydrogen bonding network, creating more continuous proton transfer pathways. Consequently, excellent proton conductivity of 0.112 S cm^{-1} and H_2-O_2 fuel cell peak power density of 980 mW cm^{-2} at 160 °C were achieved. In durability tests, the voltage decay rate of p-OPBI-ATMP/PA was only 5.46 μV h^{-1}, far superior to the unmodified porous OPBI membrane (Figure 8d).

For the three-layered membrane designed by Kannan et al.,[121] the central PBI membrane layer was directly casted from PA and acted as an acid reservoir, the outer layers were post-doped with PA and served as barriers to limit acid transport out of the central layer. During the period of 10000 h constant current operation at 200 mA cm^{-2} and 180 °C, the cells with three-layered membranes showed voltage decay rates of 2.3 and 4.1 μV h^{-1}, in construct to 14 and 11 μV h^{-1} for cells with single-layered membranes. Besides, the acid loss rates assessed by acid collection at the fuel cell exhaust were rather comparable with the durability results, convincing the PA barrier capacity of the protect layer.

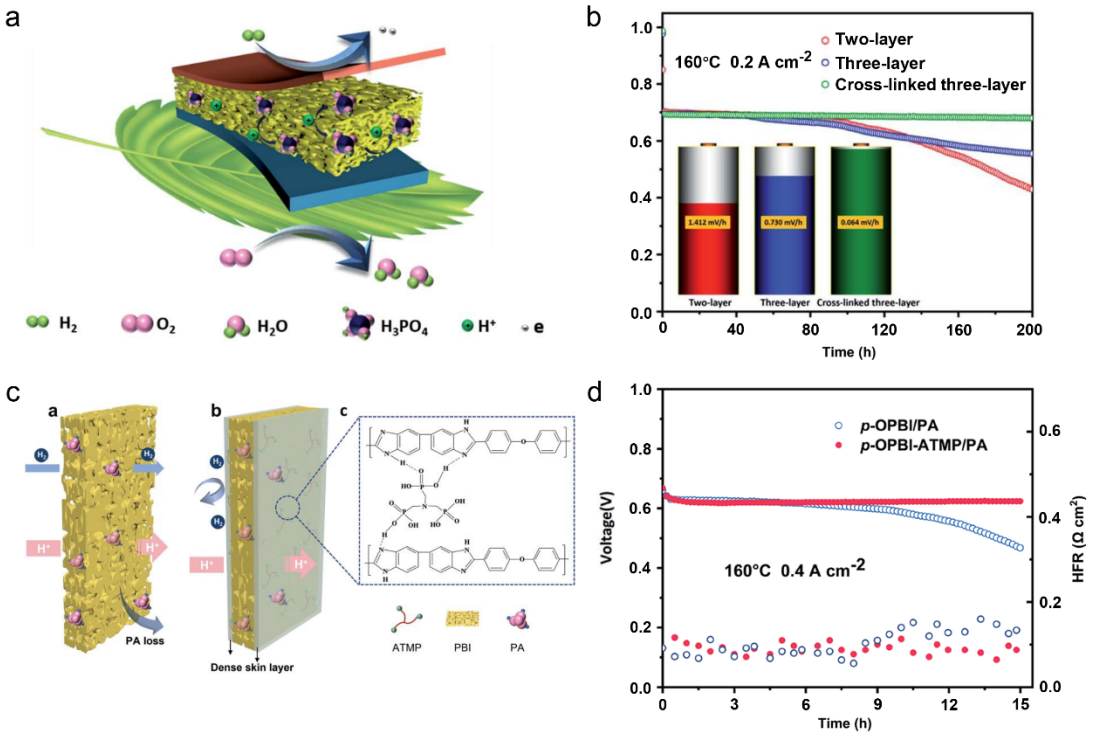

Figure 8. (**a**) Schematic diagrams of the leaf-like porous membranes and (**b**) their corresponding single-cells stabilities at 0.2 A cm^{-2} and 160 °C [119], Copyright 2022, John Wiley and Sons. (**c**) Schematic diagrams of p-OPBI-ATMP membrane and (**d**) their corresponding single-cells stabilities at 0.4 A cm^{-2} and 160 °C [120], Copyright 2021, Royal Society of Chemistry.

4. Challenges for HT-PEMs

Although the durability of PA/PBI membranes has exceeded 10,000 h, further improvement is still feasible, and durability remains the most critical performance indicator for HT-PEMFCs toward large-scale commercialization, which has attracted increasing research attention in recent years.

Mechanical degradation in FC operation, such as pinholes, perforations, cracks and tears, can originate from inherent membrane defects or inappropriate MEA fabrication. Local regions (e.g., MEA sealing edges) under excessive or non-uniform mechanical stress are susceptible to small perforations or tears [122]. Moreover, the membrane suffers in-plane tension and compression under varying load conditions [122,123]. Employing creep-resistant or mechanically robust crosslinked membranes can effectively enhance membrane durability [124–127]. Mechanical defects such as local pinholes and perforations promote reactant gas cross-permeation, ultimately triggering membrane chemical degradation. Hydrogen peroxide generated at the fuel cell electrodes decomposes into reactive HO· and HO_2· radicals, which attack the polymer backbone. Trace metal ions including Fe^{2+} and Cu^{2+} catalyze peroxide decomposition and further accelerate membrane degradation [128]. Therefore, the Fenton test is widely adopted as an ex situ accelerated method to evaluate the oxidative stability of proton exchange membranes. The membrane is immersed in 3% H_2O_2 solution containing 4 ppm Fe^{2+}, with its residual weight and chemical structure evolution monitored. Nevertheless, these tests are generally performed without phosphoric acid (PA), and both PA doping and fuel cell operation may alter polymer stability, indicating that more in-depth interpretation is required when applying the Fenton test to high-temperature proton exchange membranes.

In addition, PA loss constitutes another factor influencing long-term durability. It is widely recognized that phosphoric acid loss is mainly caused by water vapor and liquid water at the cathode [129–131]. Since the interaction energy between phosphoric acid and water is similar to that between phosphoric acid and the polymer, the large amount of water produced at the cathode during PEMFC operation can leach phosphoric acid from the membrane. Notably, numerous strategies for improving phosphoric acid retention capacity have also been reported in the preceding context. However, Benicewicz et al. [18] conducted steady-state durability testing on PA/PBI membranes for over ten thousand hours and found that phosphoric acid loss did not significantly contribute to the performance degradation over extended operation. In steady-state fuel cell durability tests within a temperature range of 80 to 160 °C, the rate of phosphoric acid loss from the membrane was less than 10 ng cm^{-2} h^{-1}, and after

40,000 h of operation, the total phosphoric acid loss was only about 2.6% of the initial amount in the MEA. The authors also performed dynamic durability testing and found that high temperatures and high loads accelerate the loss of phosphoric acid in the MEA, yet in all cases, the amount of phosphoric acid lost was relatively small compared to the total phosphoric acid present in the membrane. Besides, the impact of phosphoric acid loss should be evaluated from the perspective of the whole MEA. Holmes et al. [85] found that phosphoric acid leached from the membrane can migrate into the anode and cathode catalyst layers, forming a three-phase boundary at the membrane–catalyst interface that lowers internal resistance and benefits durability. Oono et al. [132] observed that phosphoric acid redistribution within the catalyst layers initially causes a slow voltage decay, while severe phosphoric acid depletion leads to catalyst agglomeration, reduced active surface area, and rapid voltage decline, revealing that phosphoric acid distribution strongly affects cell stability. Overall, phosphoric acid loss may not be the most decisive factor, and improving the high-temperature mechanical stability of the membrane appears to be more critical for long-term durability.

5. Conclusions and Perspectives

Significant progress has been made in high-temperature proton exchange membranes research. High-temperature proton exchange membranes employing phosphoric acid as the proton conductor exhibit favorable attributes including satisfactory proton conductivity, outstanding heat resistance and chemical stability, positioning them as the leading candidates for HT-PEMFCs. Polybenzimidazole stands out as one of the extensively researched polymer materials in this domain, and the proton transfer mechanism in polybenzimidazole membranes doped with phosphoric acid can provide insights into the fundamental principles of constructing HT-PEMs. The review summarizes various strategies to build high-efficiency and durable HT-PEMs, dividing the discussion into two sections comprised of single-component polymer membrane membranes and composite membranes.

While notable advancements have been made, challenges remain in further enhancing HT-PEM performance and durability for practical applications. To achieve reliable and long-term operation in real fuel cell systems, future research should focus on the following specific, solution-oriented directions:

(1) Although microphase separation is widely accepted to enhance proton conductivity, the nanoscale morphology and dynamic evolution of phosphoric acid-doped membranes remain largely unexplored. The distribution and migration of phosphoric acid govern not only proton conductivity but also swelling behavior and mechanical strength, which require direct nanoscale characterization and quantitative analysis.

(2) Standardized and realistic lifetime evaluation protocols for membranes under actual fuel cell operating conditions are still lacking. Moreover, the quantitative correlation between component-level degradation (e.g., membrane deterioration) and overall cell performance decay remains unclear, which hinders the rational design of durable HT-PEMFCs.

(3) Future research should adopt a holistic MEA-centered design strategy rather than optimizing individual materials separately. This includes targeted structure optimization of HT-PEMs, synergistic integration with catalyst layers, and coordinated design of key components. In particular, fundamental insights into interfacial interactions, interface stability, and intercomponent degradation mechanisms need to be systematically established.

Overall, advancing these key aspects will effectively bridge the gap between material design and real-world performance, ultimately promoting the practical deployment of high-temperature PEM fuel cells.

Author Contributions

Y.B.: methodology, formal analysis, writing—original draft, writing—review & editing; D.H.: data curation, investigation, validation; S.H.: resources, visualization; M.X.: software, validation; S.W.: conceptualization, supervision, funding acquisition, project administration. All authors have read and agreed to the published version of the manuscript.

Funding

This research was funded by the National Key Research and Development Program grant number 2018YFA0702002, and the National Key Research and Development Program (Japan-China Joint Research Program) grant number 2017YF0197900.

Institutional Review Board Statement

Not applicable.

Informed Consent Statement

Not applicable.

Data Availability Statement

No new data were created or analyzed in this study.

Conflicts of Interest

The authors declare no conflict of interest.

Use of AI and AI-Assisted Technologies

No AI tools were utilized for this paper.

References

1. Zhou, L.J.; Zhu, J.Y.; Lin, M.J.; et al. Tetra-Alkylsulfonate Functionalized Poly(Aryl Ether) Membranes with Nanosized Hydrophilic Channels for Efficient Proton Conduction. *J. Energy Chem.* **2020**, *40*, 57–64. https://doi.org/10.1016/j.jechem.2019.02.013.
2. Neelakandan, S.; Wang, L.; Zhang, B.P.; et al. Branched Polymer Materials as Proton Exchange Membranes for Fuel Cell Applications. *Polym. Rev.* **2021**, *61*, 261–295. https://doi.org/10.1080/15583724.2021.1964524.
3. Cyril, P.H.; Saravanan, G. Development of Advanced Materials for Cleaner Energy Generation through Fuel Cells. *New J. Chem.* **2020**, *44*, 19977–19995. https://doi.org/10.1039/d0nj03746j.
4. Rosli, R.E.; Sulong, A.B.; Daud, W.R.W.; et al. A Review of High-Temperature Proton Exchange Membrane Fuel Cell (HT-PEMFC) System. *Int. J. Hydrogen Energy* **2017**, *42*, 9293–9314. https://doi.org/10.1016/j.ijhydene.2016.06.211.
5. Spendelow, J.S.; Papageorgopoulos, D.C. Progress in PEMFC MEA Component R&D at the DOE Fuel Cell Technologies Program. *Fuel Cells* **2011**, *11*, 775–786. https://doi.org/10.1002/fuce.201000189.
6. Li, Q.F.; Jensen, J.O.; Savinell, R.F.; et al. High Temperature Proton Exchange Membranes Based on Polybenzimidazoles for Fuel Cells. *Prog. Polym. Sci.* **2009**, *34*, 449–477. https://doi.org/10.1016/j.progpolymsci.2008.12.003.
7. Steele, B.C.H.; Heinzel, A. Materials for Fuel-Cell Technologies. *Nature* **2001**, *414*, 345–352.
8. Kreuer, K.D. On the Development of Proton Conducting Polymer Membranes for Hydrogen and Methanol Fuel Cells. *J. Membr. Sci.* **2001**, *185*, 29–39.
9. Yang, J.S.; Wang, Y.H.; Yang, G.H.; et al. New Anhydrous Proton Exchange Membranes Based on Fluoropolymers Blend Imidazolium Poly(Aromatic Ether Ketone)s for High Temperature Polymer Electrolyte Fuel Cells. *Int. J. Hydrogen Energy* **2018**, *43*, 8464–8473. https://doi.org/10.1016/j.ijhydene.2018.03.128.
10. Li, Q.; He, R.; Jensen, J.O.; et al. PBI-Based Polymer Membranes for High Temperature Fuel Cells—Preparation, Characterization and Fuel Cell Demonstration. *Fuel Cells* **2004**, *4*, 147–159. https://doi.org/10.1002/fuce.200400020.
11. Bouchet, R.; Siebert, E. Proton Conduction in Acid Doped Polybenzimidazole. *Solid State Ionics* **1999**, *118*, 287–299. https://doi.org/10.1016/S0167-2738(98)00466-4.
12. Samms, S.R.; Wasmus, S.; Savinell, R.F. Thermal Stability of Proton Conducting Acid Doped Polybenzimidazole in Simulated Fuel Cell Environments. *J. Electrochem. Soc.* **1996**, *143*, 1225. https://doi.org/10.1149/1.1836621.
13. Haider, R.; Wen, Y.C.; Ma, Z.F.; et al. High Temperature Proton Exchange Membrane Fuel Cells: Progress in Advanced Materials and Key Technologies. *Chem. Soc. Rev.* **2021**, *50*, 1138–1187. https://doi.org/10.1039/d0cs00296h.
14. Peng, J.W.; Fu, X.Z.; Luo, J.L.; et al. Fabrication of High Performance High-Temperature Proton Exchange Membranes through Constructing Stable Cation-Rich Domain in Polybenzimidazole Membrane. *Chem. Eng. J.* **2023**, *453*, 139609. https://doi.org/10.1016/j.cej.2022.139609.
15. Qu, E.L.; Hao, X.F.; Xiao, M.; et al. Proton Exchange Membranes for High Temperature Proton Exchange Membrane Fuel Cells: Challenges and Perspectives. *J. Power Sources* **2022**, *533*, 231386. https://doi.org/10.1016/j.jpowsour.2022.231386.
16. Zhang, J.; Xie, Z.; Zhang, J.; et al. High Temperature PEM Fuel Cells. *J. Power Sources* **2006**, *160*, 872–891. https://doi.org/10.1016/j.jpowsour.2006.05.034.
17. Bose, S.; Kuila, T.; Nguyen, T.X.L.; et al. Polymer Membranes for High Temperature Proton Exchange Membrane Fuel Cell: Recent Advances and Challenges. *Prog. Polym. Sci.* **2011**, *36*, 813–843. https://doi.org/10.1016/j.progpolymsci.2011.01.003.
18. Yu, S.; Xiao, L.; Benicewicz, B.C. Durability Studies of PBI-Based High Temperature PEMFCs. *Fuel Cells* **2008**, *8*, 165–174. https://doi.org/10.1002/fuce.200800024.
19. Melchior, J.P.; Majer, G.; Kreuer, K.D. Why Do Proton Conducting Polybenzimidazole Phosphoric Acid Membranes Perform Well in High-Temperature PEM Fuel Cells? *Phys. Chem. Chem. Phys.* **2016**, *19*, 601–612. https://doi.org/10.1039/c6cp05331a.

20. Li, Q.F.; He, R.H.; Berg, R.W.; et al. Water Uptake and Acid Doping of Polybenzimidazoles as Electrolyte Membranes for Fuel Cells. *Solid State Ionics* **2004**, *168*, 177–185. https://doi.org/10.1016/j.ssi.2004.02.013.
21. Bouchet, R.; Miller, S.; Duclot, M.; et al. A Thermodynamic Approach to Proton Conductivity in Acid-Doped Polybenzimidazole. *Solid State Ionics* **2001**, *145*, 69–78. https://doi.org/10.1016/S0167-2738(01)00915-8.
22. Hughes, C.E.; Haufe, S.; Angerstein, B.; et al. Probing Structure and Dynamics in Poly[2,2′-(m-phenylene)-5,5′-bibenzimidazole] Fuel Cells with Magic-Angle Spinning NMR. *J. Phys. Chem. B* **2004**, *108*, 13626–13631. https://doi.org/10.1021/jp047607c.
23. Ma, Y.L.; Wainright, J.S.; Litt, M.H.; et al. Conductivity of PBI Membranes for High-Temperature Polymer Electrolyte Fuel Cells. *J. Electrochem. Soc.* **2004**, *151*, A8–A16. https://doi.org/10.1149/1.1630037.
24. Asensio, J.A.; Sanchez, E.M.; Gomez-Romero, P. Proton-Conducting Membranes Based on Benzimidazole Polymers for High-Temperature PEM Fuel Cells. A Chemical Quest. *Chem. Soc. Rev.* **2010**, *39*, 3210–3239. https://doi.org/10.1039/b922650h.
25. Bu, F.Z.; Zhang, Y.R.; Hong, L.H.; et al. 1,2,4-Triazole Functionalized Poly(Arylene Ether Ketone) for High Temperature Proton Exchange Membrane with Enhanced Oxidative Stability. *J. Membr. Sci.* **2018**, *545*, 167–175. https://doi.org/10.1016/j.memsci.2017.09.072.
26. He, R.H.; Li, Q.F.; Xiao, G.; et al. Proton Conductivity of Phosphoric Acid Doped Polybenzimidazole and Its Composites with Inorganic Proton Conductors. *J. Membr. Sci.* **2003**, *226*, 169–184. https://doi.org/10.1016/j.memsci.2003.09.002.
27. Subianto, S. Recent Advances in Polybenzimidazole/Phosphoric Acid Membranes for High-Temperature Fuel Cells. *Polym. Int.* **2014**, *63*, 1134–1144.
28. Zhang, J.; Zhang, J.; Bai, H.; et al. A New High Temperature Polymer Electrolyte Membrane Based on Tri-Functional Group Grafted Polysulfone for Fuel Cell Application. *J. Membr. Sci.* **2019**, *572*, 496–503. https://doi.org/10.1016/j.memsci.2018.11.035.
29. Li, X.B.; Wang, P.; Liu, Z.C.; et al. Arylether-Type Polybenzimidazoles Bearing Benzimidazolyl Pendants for High-Temperature Proton Exchange Membrane Fuel Cells. *J. Power Sources* **2018**, *393*, 99–107. https://doi.org/10.1016/j.jpowsour.2018.05.011.
30. Jiang, J.Q.; Li, Z.; Xiao, M.; et al. Quaternary Ammonium-Biphosphate Ion-Pair Based Copolymers with Continuous H^+ Transport Channels for High-Temperature Proton Exchange Membrane. *J. Membr. Sci.* **2022**, *660*, 120878. https://doi.org/10.1016/j.memsci.2022.120878.
31. Tang, H.; Geng, K.; Wu, L.; et al. Fuel Cells with an Operational Range of –20 °C to 200 °C Enabled by Phosphoric Acid-Doped Intrinsically Ultramicroporous Membranes. *Nat. Energy* **2022**, *7*, 153–162. https://doi.org/10.1038/s41560-021-00956-w.
32. Wang, L.; Ni, J.P.; Liu, D.; et al. Effects of Branching Structures on the Properties of Phosphoric Acid-Doped Polybenzimidazole as a Membrane Material for High-Temperature Proton Exchange Membrane Fuel Cells. *Int. J. Hydrogen Energy* **2018**, *43*, 16694–16703. https://doi.org/10.1016/j.ijhydene.2018.06.181.
33. Wang, L.; Wu, Y.N.; Fang, M.L.; et al. Synthesis and Preparation of Branched Block Polybenzimidazole Membranes with High Proton Conductivity and Single-Cell Performance for Use in High Temperature Proton Exchange Membrane Fuel Cells. *J. Membr. Sci.* **2020**, *602*, 117981. https://doi.org/10.1016/j.memsci.2020.117981.
34. Hu, M.S.; Li, T.Y.; Neelakandan, S.; et al. Cross-Linked Polybenzimidazoles Containing Hyperbranched Cross-Linkers and Quaternary Ammoniums as High-Temperature Proton Exchange Membranes: Enhanced Stability and Conductivity. *J. Membr. Sci.* **2020**, *593*, 117435. https://doi.org/10.1016/j.memsci.2019.117435.
35. Wang, L.; Liu, Z.R.; Liu, Y.; et al. Crosslinked Polybenzimidazole Containing Branching Structure with No Sacrifice of Effective N-H Sites: Towards High-Performance High-Temperature Proton Exchange Membranes for Fuel Cells. *J. Membr. Sci.* **2019**, *583*, 110–117. https://doi.org/10.1016/j.memsci.2019.04.030.
36. Peng, J.; Wang, S.; Fu, X.; et al. Achieving over 1000 mW cm^{-2} Power Density Based on Locally High-Density Cross-Linked Polybenzimidazole Membrane Containing Pillar[5]arene Bearing Multiple Alkyl Bromide as a Cross-Linker. *Adv. Funct. Mater.* **2022**, *33*, 2212464. https://doi.org/10.1002/adfm.202212464.
37. Hao, X.; Li, Z.; Xiao, M.; et al. Intermolecular Acid-Base-Pairs Containing Poly(p-Terphenyl-co-Isatin Piperidinium) for High Temperature Proton Exchange Membrane Fuel Cells. *Energy Environ. Mater.* **2023**, *6*, e12621. https://doi.org/10.1002/eem2.12621.
38. Lee, K.-S.; Maurya, S.; Kim, Y.S.; et al. Intermediate Temperature Fuel Cells via an Ion-Pair Coordinated Polymer Electrolyte. *Energy Environ. Sci.* **2018**, *11*, 979–987. https://doi.org/10.1039/c7ee03595k.
39. Maity, S.; Jana, T. Soluble Polybenzimidazoles for PEM: Synthesized from Efficient, Inexpensive, Readily Accessible Alternative Tetraamine Monomer. *Macromolecules* **2013**, *46*, 6814–6823. https://doi.org/10.1021/ma401404c.
40. Kim, S.-K.; Kim, T.-H.; Ko, T.; et al. Cross-Linked Poly(2,5-benzimidazole) Consisting of Wholly Aromatic Groups for High-Temperature PEM Fuel Cell Applications. *J. Membr. Sci.* **2011**, *373*, 80–88. https://doi.org/10.1016/j.memsci.2011.02.039.

41. Wang, Q.; Zhang, S.; Guo, Y.; et al. High-Performance Poly(Aromatic Pyridine) Copolymers with Crown Ether Moieties for High Temperature Polymer Electrolyte Membrane Fuel Cells. *Sci. China Chem.* **2025**, *68*, 1078–1090.
42. Wang, L.; Chen, S.; Wang, Q.; et al. Long-Durability Poly(Dibenzofuran-co-Terphenyl N-Methylimidazole) Copolymer Membranes for High-Temperature Polymer Electrolyte Membrane Fuel Cells. *Macromolecules* **2025**, *58*, 5344–5355.
43. Lee, K.S.; Spendelow, J.S.; Choe, Y.K.; et al. An Operationally Flexible Fuel Cell Based on Quaternary Ammonium-Biphosphate Ion Pairs. *Nat. Energy* **2016**, *1*, 16120. https://doi.org/10.1038/nenergy.2016.120.
44. Chen, H.; Wang, S.; Liu, F.; et al. Base-Acid Doped Polybenzimidazole with High Phosphoric Acid Retention for HT-PEMFC Applications. *J. Membr. Sci.* **2020**, *596*, 117722. https://doi.org/10.1016/j.memsci.2019.117722.
45. Tao, P.P.; Dai, Y.; Chen, S.S.; et al. Hyperbranched Polyamidoamine Modified High Temperature Proton Exchange Membranes Based on PTFE Reinforced Blended Polymers. *J. Membr. Sci.* **2020**, *604*, 118004. https://doi.org/10.1016/j.memsci.2020.118004.
46. Anahidzade, N.; Abdolmaleki, A.; Dinari, M.; et al. Metal-Organic Framework Anchored Sulfonated Poly(Ether Sulfone) as a High Temperature Proton Exchange Membrane for Fuel Cells. *J. Membr. Sci.* **2018**, *565*, 281–292. https://doi.org/10.1016/j.memsci.2018.08.037.
47. Tang, Q.W.; Yuan, S.S.; Cai, H.Y. High-Temperature Proton Exchange Membranes from Microporous Polyacrylamide Caged Phosphoric Acid. *J. Mater. Chem. A* **2013**, *1*, 630–636. https://doi.org/10.1039/c2ta00116k.
48. Ni, J.P.; Hu, M.S.; Liu, D.; et al. Synthesis and Properties of Highly Branched Polybenzimidazoles as Proton Exchange Membranes for High-Temperature Fuel Cells. *J. Mater. Chem. C* **2016**, *4*, 4814–4821. https://doi.org/10.1039/c6tc00862c.
49. Li, T.Y.; Yang, J.Y.; Chen, Q.X.; et al. Construction of Highly Conductive Cross-Linked Polybenzimidazole-Based Networks for High-Temperature Proton Exchange Membrane Fuel Cells. *Materials* **2023**, *16*, 1932. https://doi.org/10.3390/ma16051932.
50. Yang, J.S.; Jiang, H.X.; Gao, L.P.; et al. Fabrication of Crosslinked Polybenzimidazole Membranes by Trifunctional Crosslinkers for High Temperature Proton Exchange Membrane Fuel Cells. *Int. J. Hydrogen Energy* **2018**, *43*, 3299–3307. https://doi.org/10.1016/j.ijhydene.2017.12.141.
51. Li, X.B.; Ma, H.W.; Wang, P.; et al. Highly Conductive and Mechanically Stable Imidazole-Rich Cross-Linked Networks for High-Temperature Proton Exchange Membrane Fuel Cells. *Chem. Mater.* **2020**, *32*, 1182–1191. https://doi.org/10.1021/acs.chemmater.9b04321.
52. Harilal; Nayak, R.; Ghosh, P.C.; et al. Cross-Linked Polybenzimidazole Membrane for PEM Fuel Cells. *ACS Appl. Polym. Mater.* **2020**, *2*, 3161–3170. https://doi.org/10.1021/acsapm.0c00350.
53. Hu, M.S.; Ni, J.P.; Zhang, B.P.; et al. Crosslinked Polybenzimidazoles Containing Branching Structure as Membrane Materials with Excellent Cell Performance and Durability for Fuel Cell Applications. *J. Power Sources* **2018**, *389*, 222–229. https://doi.org/10.1016/j.jpowsour.2018.04.025.
54. Wu, Y.; Liu, X.; Yang, F.; et al. Achieving High Power Density and Excellent Durability for High Temperature Proton Exchange Membrane Fuel Cells Based on Crosslinked Branched Polybenzimidazole and Metal-Organic Frameworks. *J. Membr. Sci.* **2021**, *630*, 119288. https://doi.org/10.1016/j.memsci.2021.119288.
55. Peng, J.; Fu, X.; Luo, J.; et al. Constructing Novel Cross-Linked Polybenzimidazole Network for High-Performance High-Temperature Proton Exchange Membrane. *J. Membr. Sci.* **2022**, *643*, 120037. https://doi.org/10.1016/j.memsci.2021.120037.
56. Tian, X.; Wang, S.; Li, J.S.; et al. Benzimidazole Grafted Polybenzimidazole Cross-Linked Membranes with Excellent PA Stability for High-Temperature Proton Exchange Membrane Applications. *Appl. Surf. Sci.* **2019**, *465*, 332–339. https://doi.org/10.1016/j.apsusc.2018.09.170.
57. Jang, S.; Kim, S.Y.; Jung, H.Y.; et al. Phosphonated Polymers with Fine-Tuned Ion Clustering Behavior: Toward Efficient Proton Conductors. *Macromolecules* **2018**, *51*, 1120–1128. https://doi.org/10.1021/acs.macromol.7b02449.
58. Jung, H.Y.; Kim, S.Y.; Kim, O.; et al. Effect of the Protogenic Group on the Phase Behavior and Ion Transport Properties of Acid-Bearing Block Copolymers. *Macromolecules* **2015**, *48*, 6142–6152. https://doi.org/10.1021/acs.macromol.5b01237.
59. Rager, T.; Schuster, M.; Steininger, H.; et al. Poly(1,3-phenylene-5-phosphonic acid), a Fully Aromatic Polyelectrolyte with High Ion Exchange Capacity. *Adv. Mater.* **2007**, *19*, 3317–3321. https://doi.org/10.1002/adma.200602788.
60. Atanasov, V.; Kerres, J. ETFE-g-Pentafluorostyrene: Functionalization and Proton Conductivity. *Eur. Polym. J.* **2015**, *63*, 168–176. https://doi.org/10.1016/j.eurpolymj.2014.12.017.
61. Abouzari-Lotf, E.; Ghassemi, H.; Mehdipour-Ataei, S.; et al. Phosphonated Polyimides: Enhancement of Proton Conductivity at High Temperatures and Low Humidity. *J. Membr. Sci.* **2016**, *516*, 74–82. https://doi.org/10.1016/j.memsci.2016.06.009.
62. Song, M.K.; Li, H.; Li, J.; et al. Tetrazole-Based, Anhydrous Proton Exchange Membranes for Fuel Cells. *Adv. Mater.* **2014**, *26*, 1277–1282. https://doi.org/10.1002/adma.201304121.

63. Moorthy, S.; Sivasubramanian, G.; Kannaiyan, D.; et al. Neoteric Advancements in Polybenzimidazole Based Polymer Electrolytes for High-Temperature Proton Exchange Membrane Fuel Cells—A Versatile Review. *Int. J. Hydrogen Energy* **2023**, *48*, 28103–28118. https://doi.org/10.1016/j.ijhydene.2023.04.005.
64. Bakangura, E.; Wu, L.; Ge, L.; et al. Mixed Matrix Proton Exchange Membranes for Fuel Cells: State of the Art and Perspectives. *Prog. Polym. Sci.* **2016**, *57*, 103–152. https://doi.org/10.1016/j.progpolymsci.2015.11.004.
65. Guo, Z.M.; Perez-Page, M.; Chen, J.N.; et al. Recent Advances in Phosphoric Acid–Based Membranes for High–Temperature Proton Exchange Membrane Fuel Cells. *J. Energy Chem.* **2021**, *63*, 393–429. https://doi.org/10.1016/j.jechem.2021.06.024.
66. Venugopalan, G.; Chang, K.; Nijoka, J.; et al. Stable and Highly Conductive Polycation-Polybenzimidazole Membrane Blends for Intermediate Temperature Polymer Electrolyte Membrane Fuel Cells. *ACS Appl. Energy Mater.* **2020**, *3*, 573–585. https://doi.org/10.1021/acsaem.9b01802.
67. Taherkhani, Z.; Abdollahi, M.; Sharif, A. Proton Conducting Porous Membranes Based on Poly(Benzimidazole) and Poly(Acrylic Acid) Blends for High Temperature Proton Exchange Membranes. *Solid State Ionics* **2019**, *337*, 122–131. https://doi.org/10.1016/j.ssi.2019.04.019.
68. Wang, S.; Zhu, T.; Shi, B.; et al. Porous Organic Polymer with High-Density Phosphoric Acid Groups as Filler for Hybrid Proton Exchange Membranes. *J. Membr. Sci.* **2023**, *666*, 121147. https://doi.org/10.1016/j.memsci.2022.121147.
69. Bai, Y.; Xiao, M.; Huang, Z.; et al. Ionically Crosslinked Composite Membranes from Polybenzimidazole and Sulfonated Poly(Fluorenyl Ether Ketone) for High-Temperature PEM Fuel Cells. *J. Electrochem. Soc.* **2021**, *168*, 114509. https://doi.org/10.1149/1945-7111/ac35cf.
70. Mack, F.; Aniol, K.; Ellwein, C.; et al. Novel Phosphoric Acid-Doped PBI-Blends as Membranes for High-Temperature PEM Fuel Cells. *J. Mater. Chem. A* **2015**, *3*, 10864–10874. https://doi.org/10.1039/c5ta01337b.
71. Kerres, J.; Schonberger, F.; Chromik, A.; et al. Partially Fluorinated Arylene Polyethers and Their Ternary Blend Membranes with PBI and H_3PO_4. Part I. Synthesis and Characterisation of Polymers and Binary Blend Membranes. *Fuel Cells* **2008**, *8*, 175–187. https://doi.org/10.1002/fuce.200800011.
72. Suzuki, K.; Iizuka, Y.; Tanaka, M.; et al. Phosphoric Acid-Doped Sulfonated Polyimide and Polybenzimidazole Blend Membranes: High Proton Transport at Wide Temperatures under Low Humidity Conditions Due to New Proton Transport Pathways. *J. Mater. Chem.* **2012**, *22*, 23767–23772. https://doi.org/10.1039/c2jm34529c.
73. Liu, D.; Tanaka, M.; Kawakami, H. Preparation and Characterization of Phosphoric Acid-Doped Blend Membrane Composed of Sulfonated Poly(Arylene Ether Sulfone) and for Fuel Cell Application. *J. Photopolym. Sci. Technol.* **2015**, *28*, 181–186. https://doi.org/10.2494/photopolymer.28.181.
74. Hao, X.F.; Li, Z.; Xiao, M.; et al. A Phosphonated Phenol-Formaldehyde-Based High-Temperature Proton Exchange Membrane with Intrinsic Protonic Conductors and Proton Transport Channels. *J. Mater. Chem. A* **2022**, *10*, 10916–10925. https://doi.org/10.1039/d2ta00986b.
75. Guo, Z.B.; Xu, X.; Xiang, Y.; et al. New Anhydrous Proton Exchange Membranes for High-Temperature Fuel Cells Based on PVDF-PVP Blended Polymers. *J. Mater. Chem. A* **2015**, *3*, 148–155. https://doi.org/10.1039/c4ta04952g.
76. Liu, F.X.; Wang, S.; Chen, H.; et al. Cross-Linkable Polymeric Ionic Liquid Improve Phosphoric Acid Retention and Long-Term Conductivity Stability in Polybenzimidazole Based PEMs. *ACS Sustainable Chem. Eng.* **2018**, *6*, 16352–16362. https://doi.org/10.1021/acssuschemeng.8b03419.
77. Wang, P.; Li, X.; Liu, Z.; et al. Construction of Highly Conductive PBI-Based Alloy Membranes by Incorporating PIMs with Optimized Molecular Weights for High-Temperature Proton Exchange Membrane Fuel Cells. *J. Membr. Sci.* **2022**, *659*, 120790. https://doi.org/10.1016/j.memsci.2022.120790.
78. Cheng, G.; Li, Z.; Qu, E.; et al. N-H Group-Rich Dendrimer Doped Polybenzimidazole Composite Membrane with Consecutive Proton Transportation Channels for HT-PEMFCs. *Electrochim. Acta* **2022**, *434*, 141252. https://doi.org/10.1016/j.electacta.2022.141252.
79. Peng, J.W.; Wang, P.; Yin, B.B.; et al. Constructing Stable Continuous Proton Transport Channels by In-Situ Preparation of Covalent Triazine-Based Frameworks in Phosphoric Acid-Doped Polybenzimidazole for High-Temperature Proton Exchange Membranes. *J. Membr. Sci.* **2021**, *640*, 119775. https://doi.org/10.1016/j.memsci.2021.119775.
80. Chang, Y.N.; Lai, J.Y.; Liu, Y.L. Polybenzimidazole (PBI)-Functionalized Silica Nanoparticles Modified PBI Nanocomposite Membranes for Proton Exchange Membranes Fuel Cells. *J. Membr. Sci.* **2012**, *403–404*, 1–7. https://doi.org/10.1016/j.memsci.2012.01.043.
81. Lee, S.; Seo, K.; Ghorpade, R.V.; et al. High Temperature Anhydrous Proton Exchange Membranes Based on Chemically-Functionalized Titanium/Polybenzimidazole Composites for Fuel Cells. *Mater. Lett.* **2020**, *263*, 127167. https://doi.org/10.1016/j.matlet.2019.127167.
82. Abouzari-Lotf, E.; Zakeri, M.; Nasef, M.M.; et al. Highly Durable Polybenzimidazole Composite Membranes with Phosphonated Graphene Oxide for High Temperature Polymer Electrolyte Membrane Fuel Cells. *J. Power Sources* **2019**, *412*, 238–245. https://doi.org/10.1016/j.jpowsour.2018.11.057.

83. Ghosh, P.; Mandal, S.; Majumdar, S.; et al. Enhanced Power Generation, Faster Transient Response and Longer Durability of HT-PEMFC Using Composite Polybenzimidazole Electrolyte Membrane with Optimum rGO Loading. *Int. J. Hydrogen Energy* **2020**, *45*, 16708–16723. https://doi.org/10.1016/j.ijhydene.2020.04.124.
84. Chang, C.M.; Liu, Y.L.; Lee, Y.M. Polybenzimidazole Membranes Modified with Polyelectrolyte-Functionalized Multiwalled Carbon Nanotubes for Proton Exchange Membrane Fuel Cells. *J. Mater. Chem.* **2011**, *21*, 7480–7486. https://doi.org/10.1039/c1jm10439j.
85. Guo, Z.; Chen, J.; Byun, J.J.; et al. Insights into the Performance and Degradation of Polybenzimidazole/Muscovite Composite Membranes in High–Temperature Proton Exchange Membrane Fuel Cells. *J. Membr. Sci.* **2022**, *641*, 119868. https://doi.org/10.1016/j.memsci.2021.119868.
86. Rao, S.S.; Hande, V.R.; Sawant, S.M.; et al. Alpha-ZrP Nanoreinforcement Overcomes the Trade-off between Phosphoric Acid Dopability and Thermomechanical Properties: Nanocomposite HTPEM with Stable Fuel Cell Performance. *ACS Appl. Mater. Interfaces* **2019**, *11*, 37013–37025. https://doi.org/10.1021/acsami.9b09405.
87. Shabanikia, A.; Javanbakht, M.; Amoli, H.S.; et al. Polybenzimidazole/Strontium Cerate Nanocomposites with Enhanced Proton Conductivity for Proton Exchange Membrane Fuel Cells Operating at High Temperature. *Electrochim. Acta* **2015**, *154*, 370–378. https://doi.org/10.1016/j.electacta.2014.12.025.
88. Yang, J.; Li, X.; Shi, C.; et al. Fabrication of PBI/SPOSS Hybrid High-Temperature Proton Exchange Membranes Using SPAEK as Compatibilizer. *J. Membr. Sci.* **2021**, *620*, 118855. https://doi.org/10.1016/j.memsci.2020.118855.
89. Escorihuela, J.; Sahuquillo, O.; Garcia-Bernabe, A.; et al. Phosphoric Acid Doped Polybenzimidazole (PBI)/Zeolitic Imidazolate Framework Composite Membranes with Significantly Enhanced Proton Conductivity under Low Humidity Conditions. *Nanomaterials* **2018**, *8*, 775. https://doi.org/10.3390/nano8100775.
90. Chen, J.L.; Wang, L.; Wang, L. Highly Conductive Polybenzimidazole Membranes at Low Phosphoric Acid Uptake with Excellent Fuel Cell Performances by Constructing Long-Range Continuous Proton Transport Channels Using a Metal-Organic Framework (UIO-66). *ACS Appl. Mater. Interfaces* **2020**, *12*, 41350–41358. https://doi.org/10.1021/acsami.0c10527.
91. Runbabu, D.; Sannigrahi, A.; Jana, T. Blends of Polybenzimidazole and Poly(Vinylidene Fluoride) for Use in a Fuel Cell. *J. Phys. Chem. B* **2008**, *112*, 5305–5310. https://doi.org/10.1021/jp711860v.
92. Dai, Y.; Wang, J.; Tao, P.P.; et al. Various Hydrophilic Carbon Dots Doped High Temperature Proton Exchange Composite Membranes Based on Polyvinylpyrrolidone and Polyethersulfone. *J. Colloid Interface Sci.* **2019**, *553*, 503–511. https://doi.org/10.1016/j.jcis.2019.06.020.
93. Bai, H.J.; Wang, H.N.; Zhang, J.; et al. Simultaneously Enhancing Ionic Conduction and Mechanical Strength of Poly(Ether Sulfones)-Poly(Vinyl Pyrrolidone) Membrane by Introducing Graphitic Carbon Nitride Nanosheets for High Temperature Proton Exchange Membrane Fuel Cell Application. *J. Membr. Sci.* **2018**, *558*, 26–33. https://doi.org/10.1016/j.memsci.2018.04.039.
94. Schechter, A.; Savinell, R.F. Imidazole and 1-Methyl Imidazole in Phosphoric Acid Doped Polybenzimidazole, Electrolyte for Fuel Cells. *Solid State Ionics* **2002**, *147*, 181–187.
95. Doyle, M.; Choi, S.K.; Proulx, G. High-Temperature Proton Conducting Membranes Based on Perfluorinated Ionomer Membrane-Ionic Liquid Composites. *J. Electrochem. Soc.* **2000**, *147*, 34–37.
96. Elwan, H.A.; Mamlouk, M.; Scott, K. A Review of Proton Exchange Membranes Based on Protic Ionic Liquid/Polymer Blends for Polymer Electrolyte Membrane Fuel Cells. *J. Power Sources* **2021**, *484*, 229197. https://doi.org/10.1016/j.jpowsour.2020.229197.
97. Hao, J.; Li, X.; Yu, S.; et al. Development of Proton-Conducting Membrane Based on Incorporating a Proton Conductor 1,2,4-Triazolium Methanesulfonate into the Nafion Membrane. *J. Energy Chem.* **2015**, *24*, 199–206. https://doi.org/10.1016/s2095-4956(15)60301-1.
98. Rony, F.; Lou, J.; Ilias, S. Application of Nanoparticles in Modified Polybenzimidazole-Based High Temperature Proton Exchange Membranes. *J. Elastomers Plast.* **2023**, *55*, 1152–1170. https://doi.org/10.1177/00952443231189848.
99. Song, J.; Zhao, W.; Zhou, L.; et al. Rational Materials and Structure Design for Improving the Performance and Durability of High Temperature Proton Exchange Membranes (HT-PEMs). *Adv. Sci.* **2023**, *10*, 2303969. https://doi.org/10.1002/advs.202303969.
100. Dey, B.; Ahmad, M.W.; ALMezeni, A.; et al. Enhancing Electrical, Mechanical, and Thermal Properties of Polybenzimidazole by 3D Carbon Nanotube@Graphene Oxide Hybrid. *Compos. Commun.* **2020**, *17*, 87–96. https://doi.org/10.1016/j.coco.2019.11.012.
101. Hooshyari, K.; Moradi, M.; Salarizadeh, P. Novel Nanocomposite Membranes Based on PBI and Doped-Perovskite Nanoparticles as a Strategy for Improving PEMFC Performance at High Temperatures. *Int. J. Energy Res.* **2020**, *44*, 2617–2633. https://doi.org/10.1002/er.5001.
102. Ko, T.; Kim, K.; Lim, M.-Y.; et al. Sulfonated Poly(Arylene Ether Sulfone) Composite Membranes Having Poly(2,5-benzimidazole)-Grafted Graphene Oxide for Fuel Cell Applications. *J. Mater. Chem. A* **2015**, *3*, 20595–20606. https://doi.org/10.1039/c5ta04849d.

103. Singha, S.; Koyilapu, R.; Dana, K.; et al. Polybenzimidazole-Clay Nanocomposite Membrane for PEM Fuel Cell: Effect of Organomodifier Structure. *Polymer* **2019**, *167*, 13–20. https://doi.org/10.1016/j.polymer.2019.01.066.
104. Zhang, X.; Liu, Q.; Xia, L.; et al. Poly(2,5-benzimidazole)/Sulfonated Sepiolite Composite Membranes with Low Phosphoric Acid Doping Levels for PEMFC Applications in a Wide Temperature Range. *J. Membr. Sci.* **2019**, *574*, 282–298. https://doi.org/10.1016/j.memsci.2018.12.085.
105. Zhang, X.; Fu, X.; Yang, S.; et al. Design of Sepiolite-Supported Ionogel-Embedded Composite Membranes without Proton Carrier Wastage for Wide-Temperature-Range Operation of Proton Exchange Membrane Fuel Cells. *J. Mater. Chem. A* **2019**, *7*, 15288–15301. https://doi.org/10.1039/c9ta03666k.
106. Guo, Z.M.; Chen, J.N.; Byun, J.J.; et al. High-Performance Polymer Electrolyte Membranes Incorporated with 2D Silica Nanosheets in High-Temperature Proton Exchange Membrane Fuel Cells. *J. Energy Chem.* **2022**, *64*, 323–334. https://doi.org/10.1016/j.jechem.2021.04.061.
107. Cui, Y.; Wan, J.; Ye, Y.; et al. A Fireproof, Lightweight, Polymer-Polymer Solid-State Electrolyte for Safe Lithium Batteries. *Nano Lett.* **2020**, *20*, 1686–1692. https://doi.org/10.1021/acs.nanolett.9b04815.
108. Hu, J.; He, P.; Zhang, B.; et al. Porous Film Host-Derived 3D Composite Polymer Electrolyte for High-Voltage Solid State Lithium Batteries. *Energy Storage Mater.* **2020**, *26*, 283–289. https://doi.org/10.1016/j.ensm.2020.01.006.
109. Wan, J.; Xie, J.; Kong, X.; et al. Ultrathin, Flexible, Solid Polymer Composite Electrolyte Enabled with Aligned Nanoporous Host for Lithium Batteries. *Nat. Nanotechnol.* **2019**, *14*, 705–711. https://doi.org/10.1038/s41565-019-0465-3.
110. Cheng, G.; Li, Z.; Ren, S.; et al. A Robust Composite Proton Exchange Membrane of Sulfonated Poly(Fluorenyl Ether Ketone) with an Electrospun Polyimide Mat for Direct Methanol Fuel Cells Application. *Polymers* **2021**, *13*, 523. https://doi.org/10.3390/polym13040523.
111. Li, Y.; Hui, J.; Kawchuk, J.; et al. Composite Membranes of PVDF Nanofibers Impregnated with Nafion for Increased Fuel Concentrations in Direct Methanol Fuel Cells. *Fuel Cells* **2019**, *19*, 43–50. https://doi.org/10.1002/fuce.201800056.
112. Liu, G.; Tsen, W.-C.; Jang, S.-C.; et al. Mechanically Robust and Highly Methanol-Resistant Sulfonated Poly(Ether Ether Ketone)/Poly(Vinylidene Fluoride) Nanofiber Composite Membranes for Direct Methanol Fuel Cells. *J. Membr. Sci.* **2019**, *591*, 117321. https://doi.org/10.1016/j.memsci.2019.117321.
113. Zhao, G.; Xu, X.; Shi, L.; et al. Biofunctionalized Nanofiber Hybrid Proton Exchange Membrane Based on Acid-Base Ion-Nanochannels with Superior Proton Conductivity. *J. Power Sources* **2020**, *452*, 227839. https://doi.org/10.1016/j.jpowsour.2020.227839.
114. Li, M.; Scott, K. A Polymer Electrolyte Membrane for High Temperature Fuel Cells to Fit Vehicle Applications. *Electrochim. Acta* **2010**, *55*, 2123–2128. https://doi.org/10.1016/j.electacta.2009.11.044.
115. Lu, S.F.; Xiu, R.J.; Xu, X.; et al. Polytetrafluoroethylene (PTFE) Reinforced Poly(Ethersulphone)-Poly(Vinyl Pyrrolidone) Composite Membrane for High Temperature Proton Exchange Membrane Fuel Cells. *J. Membr. Sci.* **2014**, *464*, 1–7. https://doi.org/10.1016/j.memsci.2014.03.053.
116. Bai, Y.; Han, D.; Xiao, M.; et al. New Anhydrous Proton Exchange Membranes Based on Polypyrrolone (PPy) for High-Temperature Polymer Electrolyte Fuel Cells. *J. Power Sources* **2023**, *563*, 232823. https://doi.org/10.1016/j.jpowsour.2023.232823.
117. Lu, Y.; Chen, J.; Cui, H.; et al. Doping of Carbon Fiber into Polybenzimidazole Matrix and Mechanical Properties of Structural Carbon Fiber-Doped Polybenzimidazole Composites. *Compos. Sci. Technol.* **2008**, *68*, 3278–3284. https://doi.org/10.1016/j.compscitech.2008.08.014.
118. Cai, Y.B.; Yue, Z.Y.; Teng, X.; et al. Radiation Grafting Graphene Oxide Reinforced Polybenzimidazole Membrane with a Sandwich Structure for High Temperature Proton Exchange Membrane Fuel Cells in Anhydrous Atmosphere. *Eur. Polym. J.* **2018**, *103*, 207–213. https://doi.org/10.1016/j.eurpolymj.2018.02.020.
119. Wang, P.; Peng, J.; Yin, B.; et al. Phosphoric Acid-Doped Polybenzimidazole with a Leaf-Like Three-Layer Porous Structure as a High-Temperature Proton Exchange Membrane for Fuel Cells. *J. Mater. Chem. A* **2021**, *9*, 26345–26353. https://doi.org/10.1039/d1ta06883k.
120. Li, W.; Liu, W.; Zhang, J.; et al. Porous Proton Exchange Membrane with High Stability and Low Hydrogen Permeability Realized by Dense Double Skin Layers Constructed with Amino Tris(Methylene Phosphonic Acid). *Adv. Funct. Mater.* **2022**, *33*, 2210036. https://doi.org/10.1002/adfm.202210036.
121. Kannan, A.; Aili, D.; Cleemann, L.N.; et al. Three-Layered Electrolyte Membranes with Acid Reservoir for Prolonged Lifetime of High-Temperature Polymer Electrolyte Membrane Fuel Cells. *Int. J. Hydrogen Energy* **2020**, *45*, 1008–1017. https://doi.org/10.1016/j.ijhydene.2019.10.186.
122. Seselj, N.; Aili, D.; Celenk, S.; et al. Performance Degradation and Mitigation of High Temperature Polybenzimidazole-Based Polymer Electrolyte Membrane Fuel Cells. *Chem. Soc. Rev.* **2023**, *52*, 4046–4070. https://doi.org/10.1039/d3cs00072a.
123. Wu, J.F.; Yuan, X.Z.; Martin, J.J.; et al. A Review of PEM Fuel Cell Durability: Degradation Mechanisms and Mitigation Strategies. *J. Power Sources* **2008**, *184*, 104–119. https://doi.org/10.1016/j.jpowsour.2008.06.006.

124. Kannan, A.; Li, Q.; Cleemann, L.N.; et al. Acid Distribution and Durability of HT-PEM Fuel Cells with Different Electrode Supports. *Fuel Cells* **2018**, *18*, 103–112. https://doi.org/10.1002/fuce.201700181.
125. Molleo, M.A.; Chen, X.; Ploehn, H.J.; et al. High Polymer Content 2,5-Pyridine-Polybenzimidazole Copolymer Membranes with Improved Compressive Properties. *Fuel Cells* **2015**, *15*, 150–159. https://doi.org/10.1002/fuce.201400129.
126. Chen, X.M.; Qian, G.Q.; Molleo, M.A.; et al. High Temperature Creep Behavior of Phosphoric Acid-Polybenzimidazole Gel Membranes. *J. Polym. Sci. Part B Polym. Phys.* **2015**, *53*, 1527–1538. https://doi.org/10.1002/polb.23791.
127. Krishnan, N.N.; Konovalova, A.; Aili, D.; et al. Thermally Crosslinked Sulfonated Polybenzimidazole Membranes and Their Performance in High Temperature Polymer Electrolyte Fuel Cells. *J. Membr. Sci.* **2019**, *588*, 117218. https://doi.org/10.1016/j.memsci.2019.117218.
128. Inaba, M.; Kinumoto, T.; Kiriake, M.; et al. Gas Crossover and Membrane Degradation in Polymer Electrolyte Fuel Cells. *Electrochim. Acta* **2006**, *51*, 5746–5753. https://doi.org/10.1016/j.electacta.2006.03.008.
129. Jeong, Y.H.; Jung, J.H.; Choi, E.; et al. Colorimetric Determination of Phosphoric Acid Leakage for Phosphoric Acid-Doped Polybenzimidazole Membrane Fuel Cell Applications. *J. Power Sources* **2015**, *299*, 480–484. https://doi.org/10.1016/j.jpowsour.2015.09.015.
130. Mori, T.; Honji, A.; Kahara, T.; et al. Acid Absorbancy of an Electrode and Its Cell Performance History. *J. Electrochem. Soc.* **1988**, *135*, 1104.
131. Tang, H.; Gao, J.; Wang, Y.; et al. Phosphoric-Acid Retention in High-Temperature Proton-Exchange Membranes. *Chem. Eur. J.* **2022**, *28*, e202202064. https://doi.org/10.1002/chem.202202064.
132. Oono, Y.; Sounai, A.; Hori, M. Long-Term Cell Degradation Mechanism in High-Temperature Proton Exchange Membrane Fuel Cells. *J. Power Sources* **2012**, *210*, 366–373. https://doi.org/10.1016/j.jpowsour.2012.02.098.